SCIENCE CHINA
Earth Sciences

•PROGRESS•

August 2020 Vol.63 No.8: 1069–1091
https://doi.org/10.1007/s11430-019-9575-2

Observations and modeling of flat subduction and its geological effects

Zhiyong YAN[1,2,3,4], Lin CHEN[4*], Xiong XIONG[5], Kai WANG[3], Renxian XIE[3] & Hou Tze HSU[2,3]

[1] *MOE Key Laboratory of Fundamental Physical Quantities Measurement & Hubei Key Laboratory of Gravitation and Quantum Physics, PGMF and School of Physics, Huazhong University of Science and Technology, Wuhan 430074, China;*
[2] *Institute of Geophysics and PGMF, Huazhong University of Science and Technology, Wuhan 430074, China;*
[3] *State Key Laboratory of Geodesy and Earth's Dynamic, Institute of Geodesy and Geophysics, Chinese Academy of Sciences, Wuhan 430077, China;*
[4] *State Key Laboratory of Lithospheric Evolution, Institute of Geology and Geophysics, Chinese Academy of Sciences, Beijing 100029, China;*
[5] *Institute of Geophysics and Geomatics, China University of Geosciences, Wuhan 430074, China*

Received July 16, 2019; revised December 11, 2019; accepted January 2, 2020; published online March 27, 2020

Abstract Flat subduction refers to low-angle (<10°) or sub-horizontal subduction of oceanic slabs. Flat subduction is only recognized in ~10% of present-day subduction zones, but its impact on the behavior of the overriding plate is particularly strong. For example, flat subduction zones are typically associated with stronger earthquakes. The deformation caused by typical flat subduction will transfer from the trench to the overriding continental interior and form a broad magma belt. The formation mechanism of flat subduction has been linked to the relative buoyancy of subducted oceanic plateaus, overthrusting of the overriding plate, hydrodynamic suction, and trench retreat. However, these mechanisms remain debated. This paper systematically analyzes and summarizes previous studies on flat subduction, and outlines the possible geological effects of flat subduction, such as intracontinental orogeny and magmatism. Using examples from numerical modeling, we discuss the possible formation mechanisms. The most important factors that control the formation of flat subduction are associated with overthrusting of the overriding plate and the arrival of an oceanic plateau at the subduction zone. In addition, trench retreat is necessary to enable flat subduction. Hydrodynamic suction contributes to the reduction of the slab dip angle, but is insufficient to form flat subduction. Future numerical modeling of flat subduction should carry out three-dimensional high-resolution thermo-mechanical simulation, considering the influence of crustal eclogitization (negative buoyancy) and mantle serpentinization (positive buoyancy) of oceanic lithosphere, in combination with geological and geophysical data.

Keywords Flat subduction, Magmatism, Intracontinental orogeny, Formation mechanism, Numerical modeling

Citation: Yan Z, Chen L, Xiong X, Wang K, Xie R, Hsu H. 2020. Observations and modeling of flat subduction and its geological effects. Science China Earth Sciences, 63: 1069–1091, https://doi.org/10.1007/s11430-019-9575-2

1. Introduction

Subduction is the process by which a relatively dense (i.e., heavy) oceanic plate sinks into the deeper mantle at convergent plate boundaries. It is a main driving force of plate movement and oceanic spreading (Stern, 2002). Subduction zones are responsible for the production of new continental crust through arc magmatism, which forms in response to melting by the interaction of seawater, sediments, and oceanic crustal materials (carried by the subducting plate) with the surrounding hot mantle (Kelemen and Hanghoj, 2003; Grove et al., 2012). Ultimately, subduction zones allow material circulation and energy exchange between the different layers of the Earth's interior (Zheng et al., 2015;

* Corresponding author (email: chenlin@mail.iggcas.ac.cn)

© Science China Press and Springer-Verlag GmbH Germany, part of Springer Nature 2020

Zheng and Chen, 2016; Leng and Huang, 2018; Zheng et al., 2019).

Oceanic subduction zones could be divided into two types, Mariana type and Peru-Chile type, based on their subduction dip angle and the degree of coupling between the upper and lower plates (Uyeda and Kanamori, 1979; Uyeda, 1983), and these represent steep subduction and flat subduction, respectively (Figure 1). Mariana-type subduction zones are characterized by high-angle subduction of an old oceanic plate, a relatively narrow contact zone between the subducting slab and the overriding plate, relatively weak plate coupling, significant trench retreat and backarc extension, and widespread basaltic volcanism (Figure 1a). Peru-Chile-type subduction zones are characterized by shallow or flat subduction of a relatively young oceanic plate. This mode of subduction involves a broad contact zone between the plates, strong coupling, compression of the overriding plate, and a broad belt of active volcanism dominated by andesite (Figure 1b). Most of the subduction zones in the present world have steep subduction, and only 10% of them show flat subduction (Gutscher et al., 2000a). As shown in Figure 2, flat subduction is currently active in central Chile (Barazangi and Isacks, 1976; Marot et al., 2013), Peru (Barazangi and Isacks, 1976; Ma and Clayton, 2014), Ecuador (Beate et al., 2001), Costa Rica (Grafe et al., 2002; Gardner et al., 2013), southwestern Mexico (Suárez et al., 1990; Skinner and Clayton, 2011), Cascadia (Defant and Drummond, 1993), southeastern Alaska (Page et al., 1989; Fuis et al., 2008), and Japan (Nankai Trough) (Jarrard, 1986; Morris, 1995). In areas of flat subduction, the subducting slab extends subhorizontally for hundreds or even thousands of kilometers, possibly due to the presence of oceanic aseismic ridges, oceanic plateaus, or young oceanic lithosphere. Ongoing flat subduction is also closely linked to the distribution of intracontinental Quaternary volcanism and adakites (Figure 2; Gutscher et al., 2000a).

Flat subduction has a pronounced impact on the behavior of the overriding plate. For example, seismic activity in areas of flat subduction is stronger than in high-angle subduction zones (Cloos and Shreve, 1996; Conrad et al., 2004). The formation of many large and giant ore deposits has also been linked to flat subduction (Cao et al., 2011). In addition, it has been speculated that flat subduction played a major role during the early evolution of Earth (Vlaar, 1983, 1985; Abbott et al., 1994; Murphy et al., 1999).

The concept of flat subduction was first proposed by Barazangi and Isacks (1976), who studied seismic data along the Andes. These authors found that the subducted Nazca plate beneath Peru and central Chile is relatively flat, and is coupled to the South American plate with almost no asthe-

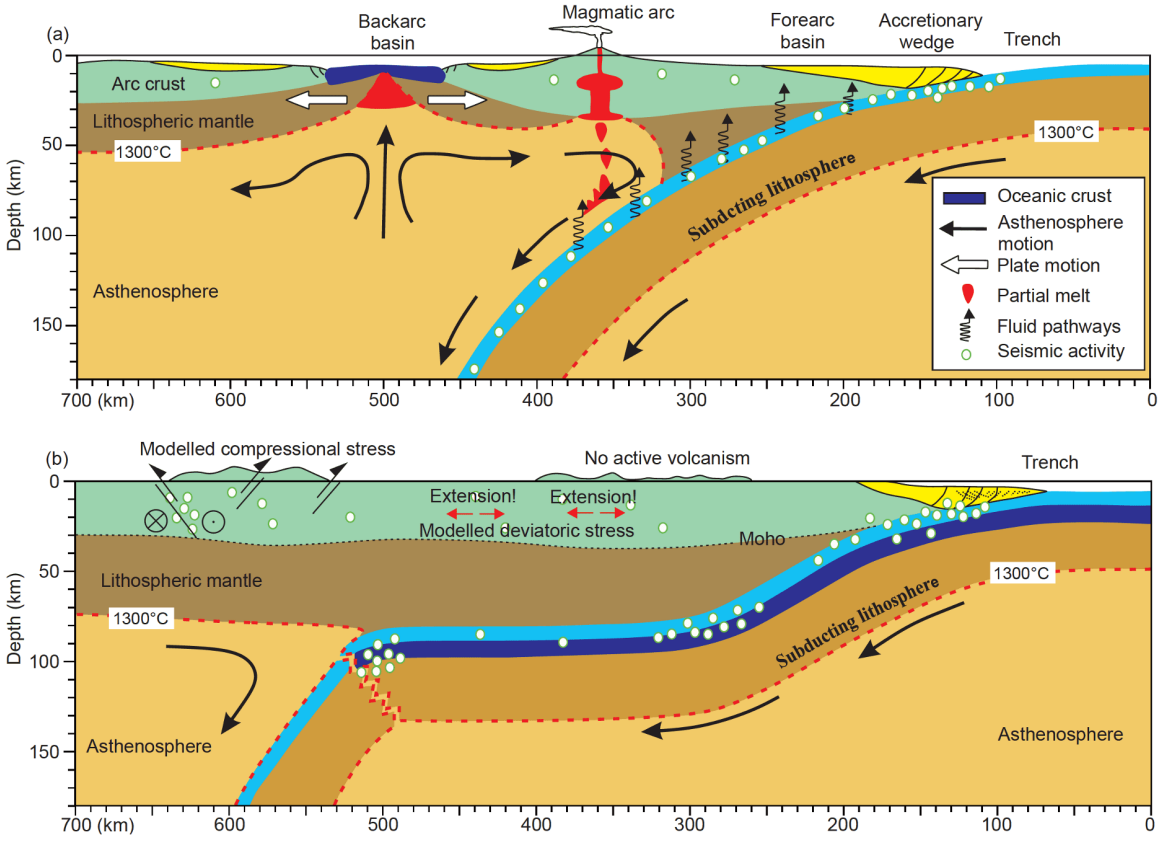

Figure 1 Two modes of subduction, (a) steep and (b) flat subduction. Modified after Barazangi and Isacks (1976), Gutscher et al. (2000b), Gutscher (2018) and Stern et al. (2017). Yellow represents accretionary wedges; light blue represents normal thickness oceanic crust; dark blue represents thickened oceanic

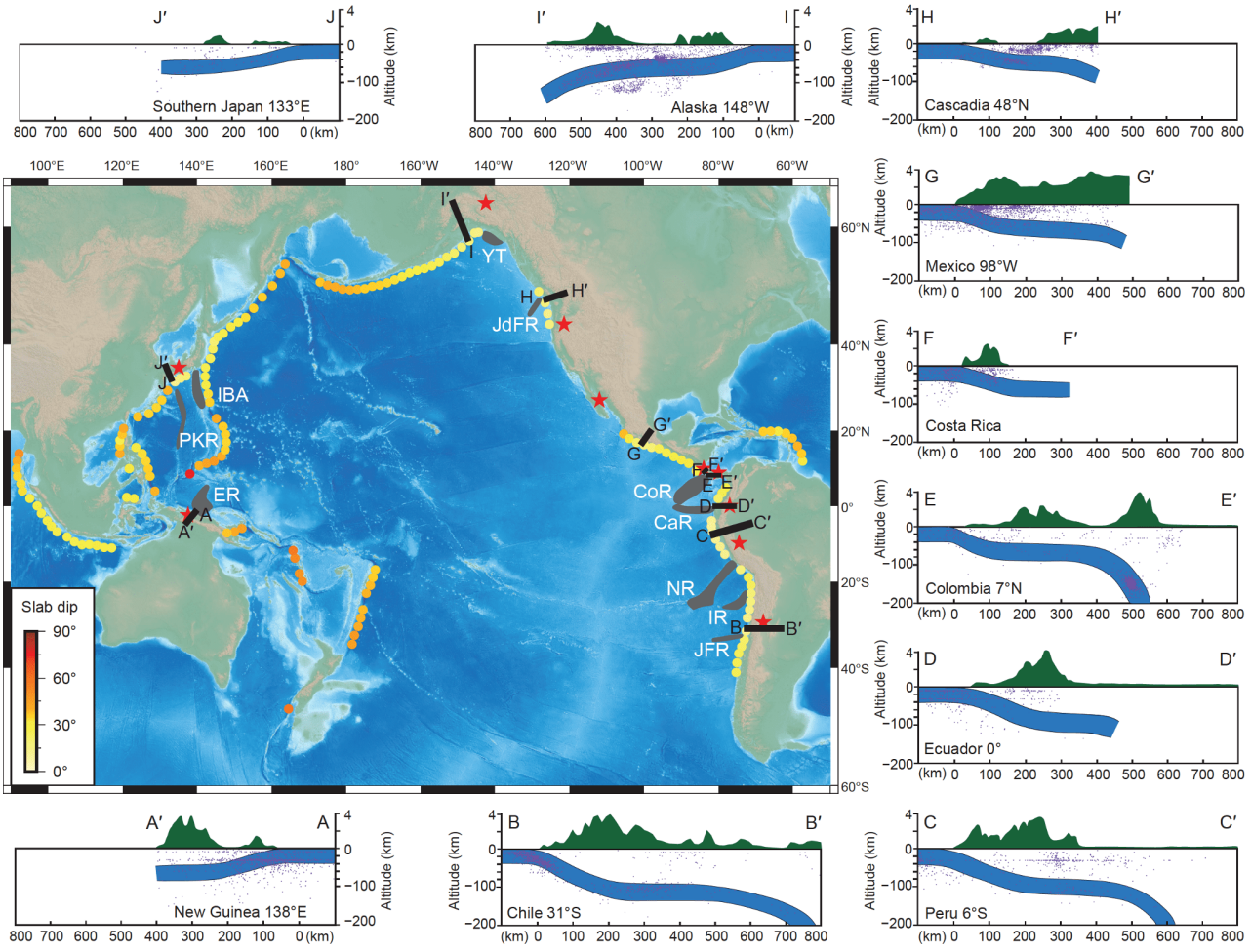

Figure 2 The current flat subduction distribution. The red pentagram represents the area where adakite is developed, the grey area represents the buoyant geological block, the purple dots represent the distribution of seismicity, and the solid black line is the profile sideline, which corresponds to the subduction structure. Subduction angle data comes from Lallemand et al. (2005), seismic distribution data comes from https://earthquake.usgs.gov/earthquakes/search/, and the time is from January 2000 to June 2019.The magnitude is 2.5–8, and the data within 1 km from the profile position is selected for mapping. Subduction structure modified after Gutscher et al. (2000a, 2000b) and Skinner and Clayton (2011). ER, Euripik Ridge; PKR, Palau-Kyushu Ridge; IBA, Izu Bonin Arc; YT, Yakutat Terrain; JdFR, Juan de Fuca Ridge; CoR, Cocos Ridge; CaR, Carnegie Ridge; NR, Nazca Ridge; IR, Iquique Ridge; JFR, Juan Fernandez Ridge.

nospheric wedge separating the two plates. In other areas along the Andes, the dip of the subducting Nazca plate is relatively steep, and the two plates are separated by the asthenosphere. The existence of flat subduction in Peru and central Chile (Barazangi and Isacks, 1976) is further supported by the recognition of gaps in arc magmatism in areas of flat subduction (Megard and Philip, 1976). A similar model has also been used to explain the Laramide orogeny in North America (80–50 Ma) (Dickinson and Snyder, 1978), which was likely driven by flat subduction of the Farallon plate (Liu et al., 2008, 2010; Liu and Gurnis, 2010; Liu and Currie, 2016; Axen et al., 2018). In the South China, flat subduction at 250–190 Ma has been used to explain the spatio-temporal distribution of magmatism and the progressive migration of the orogenic front (Li and Li, 2007). Wu et al. (2019) proposed, based on geological and geochemical data, that flat subduction of the Paleo-Pacific plate at 160–140 Ma led to the destruction of the North China Craton.

The geological effects of flat subduction are generally well understood (Gutscher, 2018), but the mechanisms that drive flat subduction are debated. The following mechanisms have been proposed: (1) anomalously buoyant material (e.g., oceanic plateaus, oceanic ridges, and seamount chains) within the subducting oceanic plate; (2) trench retreat; (3) hydrodynamic suction between the subducting and overriding plates; and (4) movement of the overriding plate towards the trench (van Hunen et al., 2004; Manea et al., 2012; Antonijevic et al., 2015). Based on a recent analysis of slab geometry, the geochemical characteristics of arc magmas, and seismic anisotropy data from three flat subduction zones (in Mexico, Peru, and Chile), Manea et al. (2017) concluded that the most important factors that control flat subduction are trench retreat, the composition of the oceanic subducting

plate, and structural heterogeneity in the overriding plate. Although no uniform mechanism had been found to explain these three flat subductions, they emphasized that the three-dimensional dynamical simulation method is an effective way to solve the mystery of flat subduction.

This paper presents a systematic analysis of the geological effects, formation mechanisms, and numerical modelling of flat subduction. Firstly, using information from previous studies, we provide a review of the dynamic process of flat subduction and its geological effects (e.g., magmatism and intracontinental orogeny). Secondly, we present three examples where flat subduction has been used to explain tectonic processes (the Laramide orogeny in North America, intracontinental orogeny in South China, and the destruction of the North China Craton). Thirdly, using information from numerical modelling, we discuss key factors that control flat subduction. Finally, we highlight outstanding problems and directions for future research.

2. Dynamics of flat subduction

2.1 Evolution of flat subduction

The evolution of flat subduction usually can be divided into three stages (Gutscher et al., 2000a; Cao et al., 2011) (Figure 3). During the first stage (Figure 3a), the slab dip angle is relatively high. When the slab reaches a depth of ~100 km, dehydration reactions within the slab lead to partial melting in the overriding asthenospheric wedge. Accordingly, a narrow calc-alkaline arc is developed ~300 km from the trench. During the second stage (Figure 3b and 3c), the arrival of anomalously buoyant oceanic lithosphere at the subduction zone (e.g., associated with relatively young oceanic crust or the presence of an oceanic plateau) leads to a gradual flattening of the slab dip angle. The slab can then lie sub-horizontally below the overriding plate, with the tongue-shaped asthenospheric wedge migrating towards the continental interior. Partial melting of the flat slab can occur at ~80 km depth, when temperatures are higher than 700°C, leading to a broad zone of adakitic magmatism located ~400 km from the trench (Figure 3b). The slab can remain sub-horizontal over a distance of several hundreds, or even thousands, of kilometers. As the tongue-shaped asthenospheric wedge between the two plates is continuously retracted and cooled, partial melting occurs at a great distance from the trench (Figure 3c). During the final stage (Figure 3d), cooling of the asthenospheric wedge results in a volcanic gap.

Previous studies have focused mainly on the evolution of flat subduction, whereas the post-flat subduction processes have received less attention. Flat subduction is a transient process, meaning that the shape of the slab can be modified during the evolution of the subduction zone. Based on geochemical and geophysical observations (Li and Li, 2007; Wu et al., 2019), as well as numerical modelling (Taramón et al., 2015; Hu et al., 2016; Axen et al., 2018), it has been suggested that the buoyancy of flat slabs could be decreased by eclogitization, thus leading to slab tear or rollback. This change in subduction mode affects the topography of the overriding plate forming, for example, intra-continental shallow sea basins (Li and Li, 2007; Wu et al., 2019), and can also lead to renewed magmatism closer to the trench (Hu et al., 2016; Axen et al., 2018). Since the previous studies have paid little attention to rock phase transitions (see Section 5.5.1 below), the post-flat subduction processes are still poorly understood. This will be a possible breakthrough in the future study of flat subduction.

2.2 Thermal structure of flat subduction

The thermal structure of the subduction zone affects the negative buoyancy of the subducting slab, seismicity, mineral phase transitions, dehydration reactions, and magmatism. Flat subduction can influence the temperature distribution and rheological properties below the continental margin, which in turn affects the deformation pattern and volcanism in the overriding plate (Gutscher et al., 2000a; Manea and Manea, 2011; Marot et al., 2014). During subduction, hot asthenosphere at the base of the overriding continental lithosphere is replaced by cold oceanic lithosphere, meaning that a large-scale cold thermal structure is expected in the case of flat subduction (Sacks, 1983; Henry and Pollack, 1988; Dumitru et al., 1991; Axen et al., 2018). According to the plate age, subduction velocity and geometrical parameters of the plate in the Andean flat subduction zone, Gutscher et al. (2000a) compiled the thermal structure of the steep subduction by finite element method (Peacock et al., 1994; Peacock, 1996) and the thermal structure of the flat subduction (below 70 km) calculated by Davies (1999) using analytical solutions together, building a complete thermal structure of the flat subduction zone for the first time. The model predicts the P-T-t path of the metamorphic reaction under flat subduction conditions, and explains the origin of the adakite in the subduction zone of South America. However, it does not consider the dynamic processes of shear heat generation, melting endotherm and advection heat transfer, thus the predicted temperature is lower than the actual. Syracuse et al. (2010) synthesized the results of previous studies and used the Sepran software package to model the temperature structure of 56 major subduction zones around the world, and obtained a complete global subduction thermal model. The results show that the subducting plate and the overriding plate of all models represent local coupling characteristics. With the same subduction model, different decoupling-point has little effect on the Moho temperature of the subducting plate, the shallow

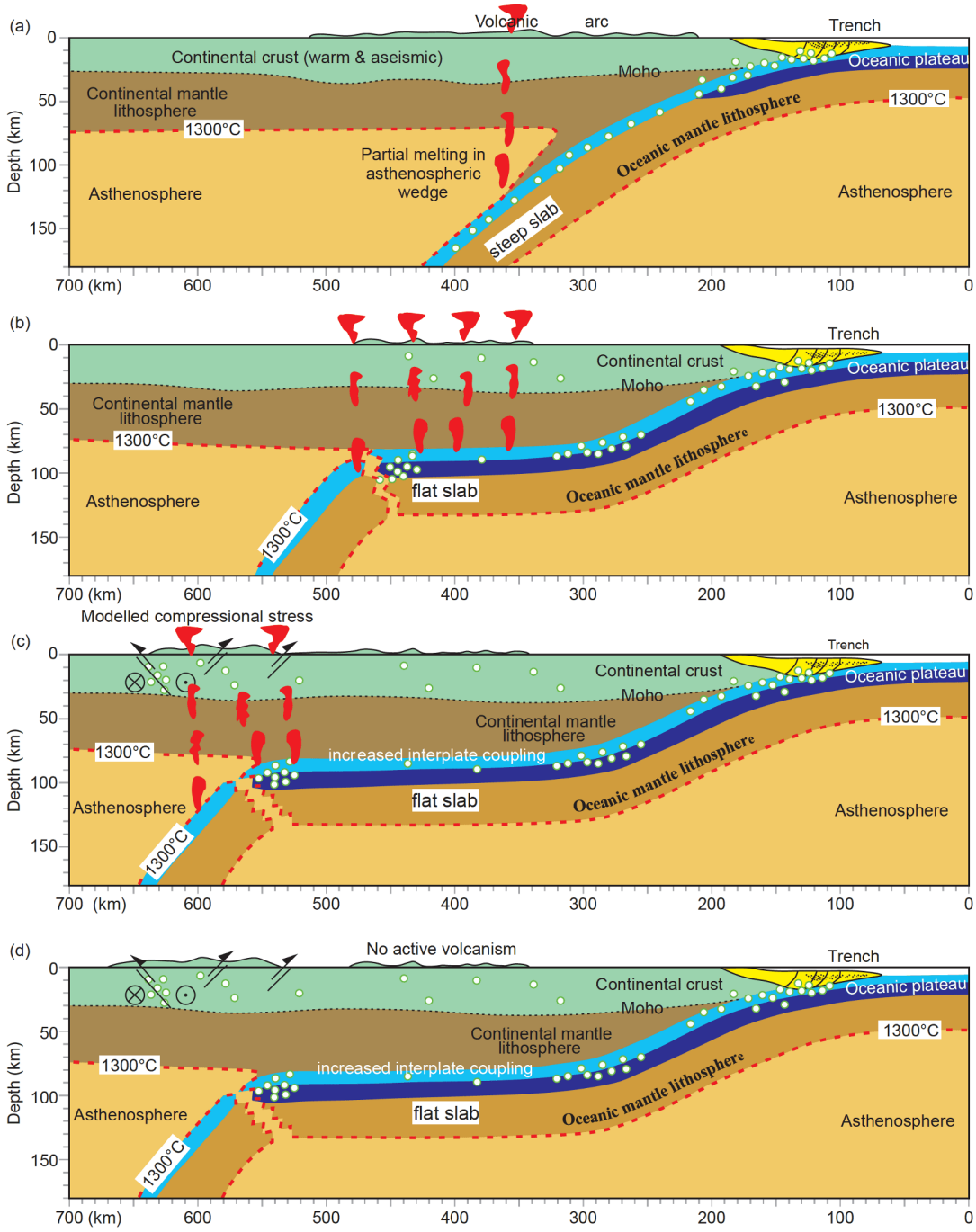

Figure 3 The first stage is the steep subduction (a), and a narrow calc-alkaline magma arc is formed above the mantle wedge. The second stage is the development process of flat subduction ((b), (c)), with the oceanic plateau entering the subduction zone, the subducting plate slipped horizontally for hundreds of kilometers along the bottom of the overriding plate, causing magma and orogeny to gradually migrate inland. The third stage is the late stage of flat subduction (d), as the disappearance of the wedge-shaped asthenosphere, a volcanic gap result.

temperature beneath the island arc, and the maximum temperature in the mantle wedge. Recently, Penniston-Dorland et al. (2015) studied the exposed blueschists and eclogites, and found that under the same pressure conditions, the thermal structure predicted by petrology experiments is hotter than that predicted by Syracuse et al. (2010) using kinematic models, especially in the shallower depth (<2 GPa) which is 100–300°C higher on average. In addition, mineral phase transitions and dehydration reactions affect the thermal structure of subduction zones (van Keken et al., 2011). Given these considerations, the thermal structure of subduction zones, and particularly flat subduction zones, remains poorly constrained.

Figure 4 shows the thermal evolution of a flat subduction zone based on the results of two-dimensional thermo-mechanical modelling (I2VIS; Gerya and Yuen, 2003). During

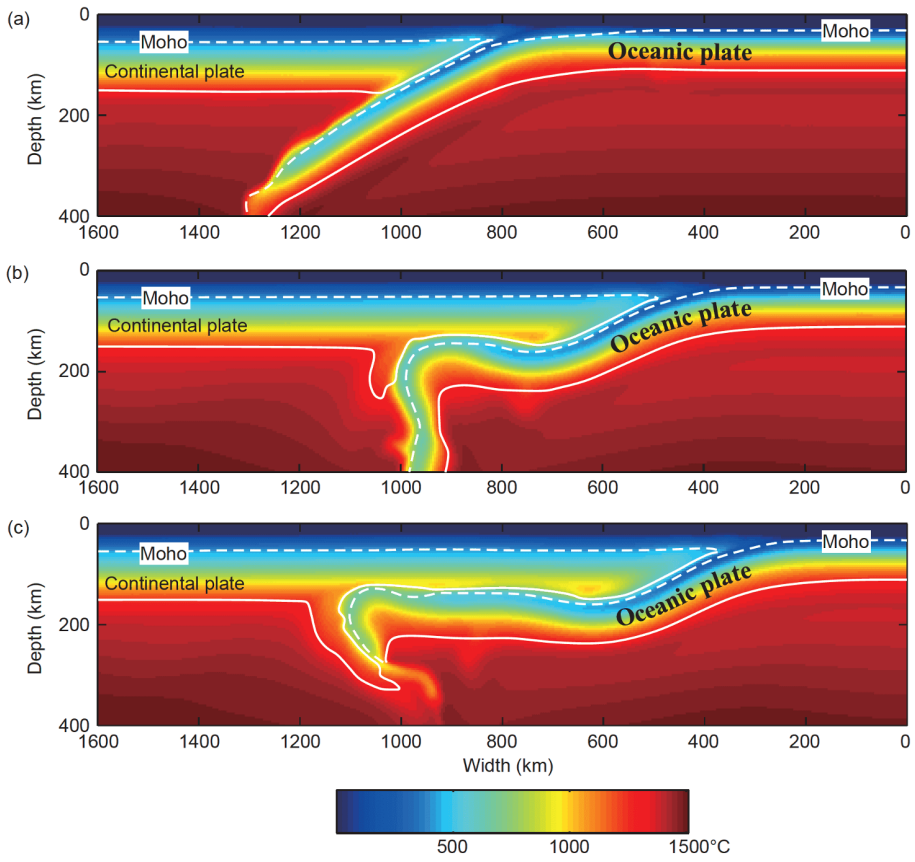

Figure 4 Thermal structure of flat subduction. The model has a horizontal width of 4000 km and a vertical depth of 1000 km. The subducting oceanic plate has an oceanic plateau with a size of 300 km. The bottom is a permeable boundary, and the remaining three sides are free sliding boundary conditions. The convergence rate is 4 cm yr^{-1}. In the figure, the white dashed line is the Moho interface; the white solid line is the lithosphere bottom interface.

the early stage of subduction, the temperature in the asthenospheric wedge is relatively high (Figure 4a). The flat subduction process leads to closure of the wedge, which is replaced by the colder subducting slab (Figure 4b and 4c). A decrease in subduction angle is accompanied by cooling of the mantle wedge. Accordingly, surface heat flow is lower above flat subduction zones. For example, in Bolivia (steep subduction), the surface heat flow is 50–120 mW m^{-2} (Henry and Pollack, 1988), whereas in Mexico and Peru (flat subduction) the heat flow is 13–22 mW m^{-2} (Ziagos et al., 1985) and 30–70 mW m^{-2} (Henry and Pollack, 1988; Muñoz, 2005), respectively. Due to the closure of the mantle wedge and the coupling between the flat slab and the overriding plate, the top of the flat slab can eventually (after a period of >5 Myr) exceed the melting temperatures that lead to adakitic magmatism. Under normal subduction conditions, adakitic magma can be generated only if the subducting oceanic lithosphere is very young (≤5 Ma) (Defant and Drummond, 1993; Peacock et al., 1994). Under the conditions of flat subduction, melting of oceanic crust can occur at the leading edge of the subducting slab and at the relatively shallow depth of flat subduction (corresponding to pressures of 2.0–2.5 GPa; Gutscher et al., 2000a). Under these conditions, adakitic magma can also be generated from melting of relatively old (40–50 Ma) oceanic lithosphere. This might explain the occurrence of adakites in the Andes and Central America. Cooling of the thermal structure in response to flat subduction will also change the rheological behavior of the subduction zone by enhancing the strength of the overriding plate. This will lead to an increase in the depth of the seismogenic layer, an increase in the energy released by earthquakes, and inboard migration of the deformation front (Gutscher et al., 2000b). The colder thermal structure will also delay the process of eclogitization (8–10 Myr later in comparison with steep subduction), thus delaying the collapse of the subduction zone and promoting further inboard movement of the slab (Gutscher et al., 2000b).

3. Geological effects of flat subduction

3.1 Magmatism

In comparison with steep subduction, magma produced by flat subduction differs in composition, spatial-temporal distribution, and metallogenesis (Table 1). In steep subduction zones, magma is produced by melting of the mantle wedge in

response to dehydration reactions in the subducting slab. In an oceanic setting, such as the western Pacific (Mariana), this magmatism gives rise to a chain of island arc volcanoes, which are typically composed of basalts and minor andesite with a relatively low value of Sr/Y. Magmatism in areas of flat subduction commonly occurs far from the trench. During flat subduction, this magmatic activity propagates towards the continental interior, forming a magmatic belt at a distance of >300 km (and even thousands of kilometers) from the trench. Numerical modelling results show that magmatic activity is likely to be dramatically weakened by flat subduction (Gerya et al., 2009; Hu et al., 2016). Volcanism associated with flat subduction consists mainly of andesite-dacite-rhyolite, with minor volumes of basalt and adakite generated by partial melting of the subducting oceanic crust. The latter is characterized by a high value of Sr/Y. Examples of such magmatic rocks are found in South America, along the Chilean flat subduction segment (Gutscher et al., 2000a; Yogodzinski et al., 2001; Zheng et al., 2015). Backarc extensional basins, associated with Mariana-type subduction zones (steep subduction), commonly host massive sulfide deposits. In contrast, porphyry deposits are commonly found in areas subjected to backarc compression in Chilean-type subduction zones (flat subduction) (Uyeda and Kanamori, 1979; Wan et al., 2017). The occurrence of adakitic magmatism is closely linked to the formation of porphyry ore deposits (Thiéblemont et al., 1997; Oyarzun et al., 2001).

Of the 10 known regions of flat subduction worldwide, 8 are linked to young (<6 Ma) adakitic magmas (indicated by stars in Figure 2; Gutscher et al., 2000a). Cenozoic adakites have been documented in many regions (Defant and Drummond, 1990; Morris, 1995), and their origin has been attributed to melting of the overriding continental crust (Kay and Abbruzzi, 1996), the formation of a slab window (Johnston and Thorkelson, 1997), and partial melting of the subducting slab (Gutscher et al., 2000a). The generation of adakitic melt in response to crustal thickening can explain the occurrence of adakites in South America. However, the thickness of the continental crust in Cascadia, southern Alaska, and southwestern Japan does not exceed 40 km (Oleskevich et al., 1999), meaning that the formation of adakites in these regions cannot be linked to the existence of an anomalously thick crust. In southern Alaska, the existence of a slab window during the Jurassic might explain the generation of adakite by partial melting of the garnet-bearing mafic basement (Cole et al., 2006). However, many other occurrences of adakites, such as in Chile and Peru (Gutscher et al., 2000a), cannot be explained by this model. Andesitic and dacitic magmas are characterized by depletion in Y and heavy rare earth elements, indicating that slab melting is a possible source of adakitic arc magma. For example, the geochemical and isotopic signature of late Miocene adakites in Mexico is characteristic of a slab-like melt, which was likely produced in response to a long period of flat subduction (Gómez-Tuena et al., 2003; Mori et al., 2007). In Ecuador and Costa Rica, spatio-temporal changes from calc-alkaline composition to adakitic magmas have been discussed in the context of subduction geometry (Defant et al., 1992; Gutscher et al., 2000a; Bourdon et al., 2003). An early stage of relatively steep subduction at Costa Rica (at 6 Ma) produced calc-alkaline magmatism, followed (at ~5 Ma) by flattening of the slab and uplift of the Talamanca Mountains in response to subduction of the Cocos Ridge (Protti et al., 1994) and melt derived from the subducting slab (Defant et al., 1992).

In Peru and central Chile, Quaternary volcanism is absent in areas of flat subduction, most likely because the mantle wedge between the subducting plate and the overriding continental plate has been removed (Gutscher, 2002; Kay and Mpodozis, 2002). These gaps in arc volcanism coincide with the spatial-temporal distribution of large and giant ore deposits (Gutscher et al., 2000a; Cao et al., 2011). Numerical simulations have shown that these flat subduction segments in South America might also coincide with tears in the subducting slab (Hu et al., 2016), thus revealing the mechanism that triggered melting.

3.2 Intracontinental orogeny

Intracontinental orogeny occurs far from the plate boundary

Table 1 Magmatism in steep and flat subduction zones

	Distance to the trench (km)	Distribution range	Lithology	Chemical composition	Metallogenic type	Typical example
Steep subduction	~300	Narrow arc	Mainly basalts and andesites. Minor dacite	Rich in Y, and low Sr/Y ratios	Massive sulphide deposits	Mariana
Flat subduction	400–700	Broad arc (300–1000 km)	Andesite-dacite-rhyolite (ADR). Mainly andesite, and minor basalts. Adakite	ADR: Rich in Y, and a low Sr/Y ratio Adakite: depleted in Y, and high Sr/Y ratios	Porphyry deposits	Chile, Peru
References	Gutscher et al. (2000a)	Gutscher et al. (2000a)	Stern (2002); Zheng et al. (2015)	Stern (2002); Oyarzun et al. (2001); Yogodzinski et al. (2001)	Zheng et al. (2015); Uyeda and Kanamori (1979); Wan et al. (2017)	Oyarzun et al. (2001); Uyeda and Kanamori (1979); Wan et al. (2017)

and therefore cannot be easily explained by subduction processes. Flat subduction, however, can extend hundreds or even thousands of kilometers from the trench, triggering deformation, crustal thickening, and uplift over a broad zone. During the evolution of a flat subduction zone, deformation is expected to migrate towards the continent (Figure 3). For example, flat subduction caused by subduction of the Juan-Fernandez Ridge resulted in shortening along the coastline of central Chile and thickening in the Sierras Pampeanas (Fromm et al., 2004). Flat subduction of the Cocos Ridge led to rapid uplift of the Osa Peninsula in southern Costa Rica (Marshall and Anderson, 1995; Gardner et al., 2013). In Ecuador, flat subduction of the Carnegie Ridge was responsible for uplift of both the forearc and backarc areas, more than 110 km from the trench (Michaud et al., 2009). Flat subduction in Peru, formed by the subduction of the Nazca Ridge, is linked to morphotectonic provinces, which are, from west to east, the forearc, the Western Cordillera, the northern part of the Altiplano, the Eastern Cordillera, and the Subandes (Ramos and Folguera, 2009; Manea et al., 2017).

Recent numerical simulations have confirmed that intracontinental orogeny can be triggered by flat subduction. For example, Gerya et al. (2009) have demonstrated that the topographic response to flat subduction migrates away from the trench during flat subduction. Similar conclusions have been drawn by Axen et al. (2018) based on numerical modelling.

3.3 Summary

The continental lithosphere overriding a flat subduction zone is typically subjected to compressive stresses. During the evolution of flat subduction, the overriding plate is subjected to compressional deformation, accompanied by crustal thickening and uplift. Magmatic activity migrates towards the continent. Altogether, flat subduction effectively transfers tectonic activity and magma activity towards the interior of the overriding plate. In a later stage of flat subduction, the hot mantle wedge is replaced by the cold subducting slab, leading to a volcanic gap. Therefore, typical flat subduction usually has the following characteristics: (1) The deformation of the overriding plate migrates to the intracontinent; (2) Island arc magma activity migrates, weakens or disappears into the intracontinent. These characteristics have also become an important geological basis for judging or speculating the flat subduction.

4. Evidence of flat subduction in the geological record

Flat subduction zones likely existed in past geological periods (Dickinson and Snyder, 1978; Li and Li, 2007). During the Archean, temperatures were higher, the oceanic crust was thicker (i.e., oceanic plates were more buoyant), and the viscosity of the mantle was lower. Accordingly, flat subduction during the Archean might have been more common than at present (Abbott et al., 1994; Murphy et al., 1999). In the following section, we discuss three examples of flat subduction from the geological record, linked to the Laramide orogeny in North America, the Mesozoic intracontinental orogeny in South China, and the destruction of the North China Craton.

4.1 Farallon flat subduction and the Laramide orogeny in North America

The Laramide orogeny in North America began in the Late Cretaceous and ended in the Oligocene. It was associated with uplift, compressional deformation, and volcanic activity that migrated 1000–1500 km towards the foreland in the western United States (Dickinson and Snyder, 1978; Rodgers, 1987; English and Johnston, 2004). A variety of mechanisms have been proposed to explain the origin of the Laramide orogeny, including: (1) backarc thrusting (Price, 1981); (2) large-scale detachment of orogenic belts (Oldow et al., 1990); (3) cordillera compression torque collision (Maxson and Tikoff, 1996); and (4) flat subduction (Dickinson and Snyder, 1978; Bird, 1988). The first three mechanisms cannot explain the origin of intracontinental deformation and the migration of magmatism towards the continent. Therefore, flat subduction is regarded as the most likely mechanism for the formation of the Laramide orogeny. Livaccari et al. (1981) have suggested that flat subduction was caused by the arrival of the Hess Ridge, which was a crustal anomaly within the Farallon plate. Henderson et al. (1984) considered the role of other ridges within the Farallon plate, which was subduction from the Late Jurassic to the Early Cretaceous. Using numerical modeling, Bird (1988) tested the hypothesis that the Laramide orogeny was triggered by flat subduction. The results showed that coupling between the flat slab and the lithospheric mantle of the North American continent was able to transmit shear stresses to the overriding plate, thus leading to foreland uplift and deformation (Bird, 1988). Murphy et al. (1998, 2003) proposed a model that combined a mantle plume with flat subduction. These authors suggested that a mantle plume was responsible for the formation of an oceanic plateau, which was subsequently subducted beneath North America, thus forming a flat slab segment. Liu et al. (2010) combined an inversion of mantle convection with a plate tectonic reconstruction of the Farallon plate since 100 Ma. According to this model, flat subduction occurred in response to the arrival at the subduction zone of the Shatsky and Hess plateaus during the Late Cretaceous. During flat subduction, eclogitization of the oceanic crust led to regional uplift associated with the Lar-

amide orogeny (Liu et al., 2010).

Axen et al. (2018) used a two-dimensional thermo-mechanical model to investigate the dynamic evolution of the Farallon plate beneath the North American continent and the formation of flat subduction (Figure 5). At an early stage of the model, subduction of the Farallon plate is characterized by a steep slab dip. Flattening of the slab commences when the conjugate Shatsky Rise (CSR) enters the subduction zone, which results in loading of the overriding plate and compression. With the breakage of the dense front-end plate, the flat subduction was further strengthened. The results of Axen et al. (2018) show that flat subduction can scrape 20–50 km of thick continental lithospheric mantle from the bottom of the overriding plate. The asthenospheric wedge is replaced by a mixture of scraped lithospheric mantle and oceanic crust, inhibiting melting of the asthenospheric wedge and eventually leading to weakening or termination of arc magmatism. The fate of the scraped material depends on its density. If it is relatively light, it can accumulate at the front of the subducting plate and form a 'bulldozed keel'. However, if it is relatively dense, it can sink with the subducting plate. The model of Axen et al. (2018) highlights the role of flat subduction in scraping the bottom of the continental lithosphere and the formation of a bulldozed keel. The model explains some of the main features of the Laramide orogeny. For example, gravity anomalies in eastern New Mexico and southwestern Texas might represent the remains of the bulldozed keel, and the 50 km thick lithosphere in southwestern Colorado might represent a remnant of the flat-slab retracement. The model of Axen et al. (2018) also predicts horizontal extension above the bulldozed keel (Figure 5b), thus explaining the rupture of the block that gradually becomes younger from west to east caused by the Laramide orogeny. At the same time, it also answers why the top of the Peruvian flat subduction is the active positive fracture rather than the compression deformation (Gutscher, 2018).

4.2 Flat subduction and intracontinental orogeny in South China

The South China Block contains three early Mesozoic orogens: (1) along the northern margin of the South China Block, the Qinling-Dabie orogenic belt records the collision with the North China Craton (Xu et al., 1992; Zhang et al., 1996); (2) the Longmenshan Belt, situated along the northwestern margin of the South China Block (Chen and Wilson, 1996), was likely developed due to collision with the Qiangtang Block (Li and Li, 2007); and (3) the South China (or Huanan) Orogenic Belt is a broad northeast-trending fold belt that covers a large area in the South China Block (Cui and Li, 1983). The latter is a 1300 km wide intracontinental orogenic belt (Li and Li, 2007) that hosts widespread late Mesozoic granites. The spatial-temporal distribution of these granites seems to correspond to the subducting plate boundary, with older granites (250–190 Ma) situated relatively close to the subduction zone (Li and Li, 2007) and younger granites (190–90 Ma) showing a pattern of southeast younging that corresponds to a migration rate of 7.5–10 km Myr^{-1} (Zhou and Li, 2000).

Various tectonic models have been proposed to explain the origin of the South China Orogenic Belt, including subduction in the western Pacific (Cui and Li, 1983), continental collision/accretion (Hsu et al., 1990), and collision between the South China Block and the North China Craton (Li, 1998). None of these models, however, explains the spatial-temporal distribution of magmatic rocks in the South China Orogenic Belt. Li and Li (2007) proposed a flat subduction model (Figure 6) in which the initial contact between the South China and North China blocks commenced in the earliest Permian (Zhao and Coe, 1987). During the middle Permian, the onset of collision between these two blocks might have triggered the initiation of an active margin along the southeastern margin of the South China Block (Li et al., 2006), leading to coastal uplift and transfer of terrestrial sediments towards the interior of the South China Block (Figure 6b). During the Triassic (Figure 6c and 6d), an oceanic plateau arrived at the subduction zone, triggering flat subduction. Flat subduction was accompanied by gradual propagation of the volcanic arc, the orogenic front, and the foreland basin towards the interior of the South China Block. During the Jurassic (Figure 6e and 6f), due to the collapse of the continental lithosphere and the reentry of the subducting plate, the lower continental lithosphere of the migratory orogenic belt was deflected, resulting in a broad basin, which was accompanied by local extension and non-orogenic magmatism.

The flat subduction model is a good explanation for the 1300 km wide intracontinental orogenic effect between 250 Ma and 190 Ma in the South China: not only explains the development of a broad (~1300 km) intracontinental orogen that migrated from the coastal region into the continental interior between ca. 250 Ma and 190 Ma, but can also account for the puzzling chain of events that followed: the formation of a shallow-marine basin in the wake of the migrating foreland fold-and-thrust belt, and the development of the foreland basin.

4.3 Destruction of the North China Craton in response to flat subduction

The Archean North China Craton was subjected to lithospheric thinning and deformation during the Mesozoic (Menzies et al., 1993; Deng et al., 1994; Griffin et al., 1998; Gao et al., 1998; Wu et al., 2008; Zheng and Wu, 2009; Xu et al., 2009; Zhu et al., 2011, 2012), and its formation mechanism has been greatly promoted (Deng et al., 1994;

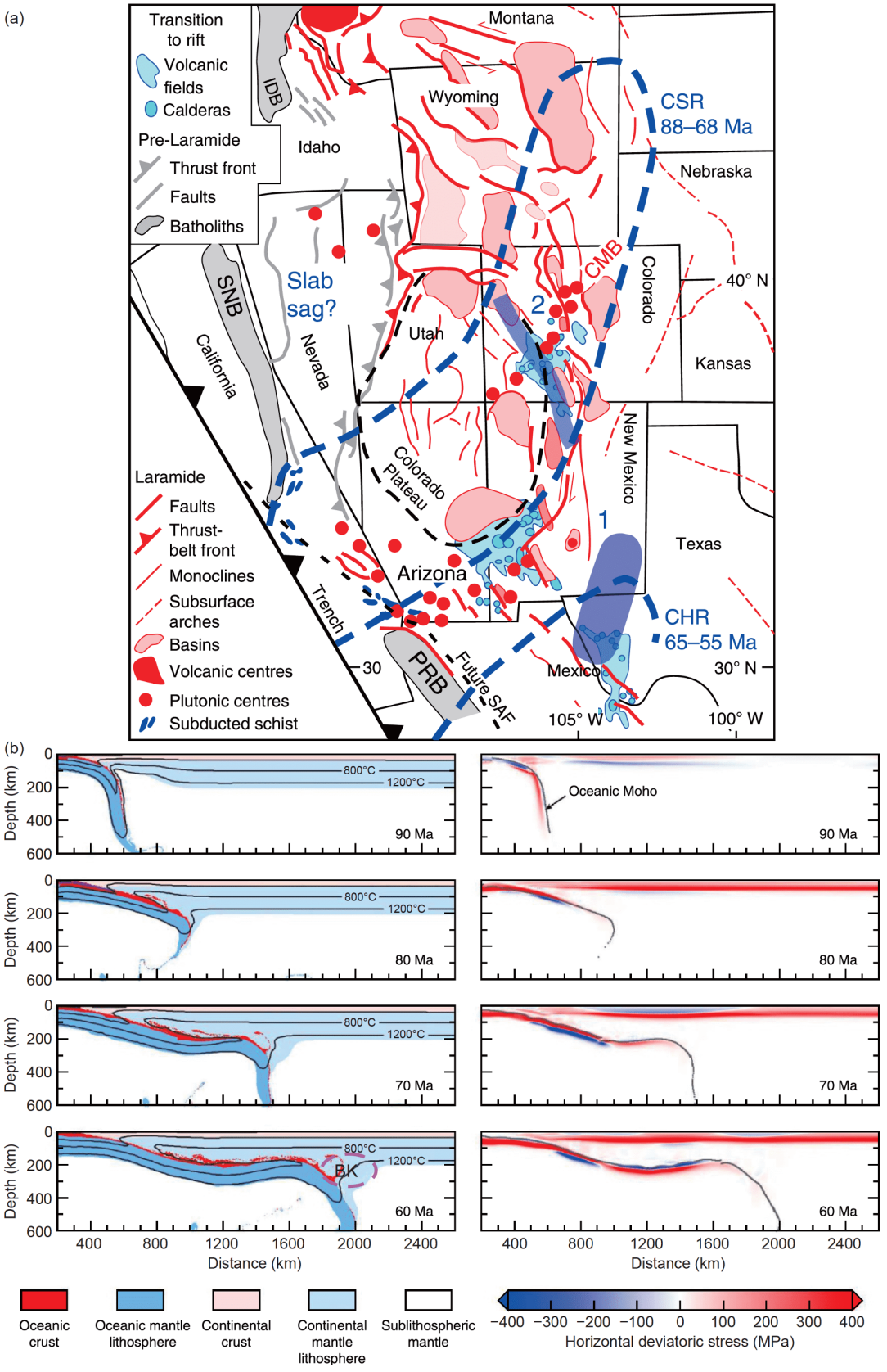

Figure 5 (a) Laramide tectonic setting in western North America, IDB, Idaho; PRB, Peninsular Ranges; SNB, Sierra Nevada. The black dashed line is the San Andreas fault and the Colorado Plateau. The blue ellipse 1 shows the high-speed upper mantle. The blue line 2 represents the lithosphere step. (b) Evolution of flat subduction (modified after Axen et al., 2018). Left, material and temperature; right, horizontal deviatoric stress (compression positive). The model with a mildly depleted (density 3230 kg m^{-3}), moderately strong (10× wet olivine). BK: bulldozed keel.

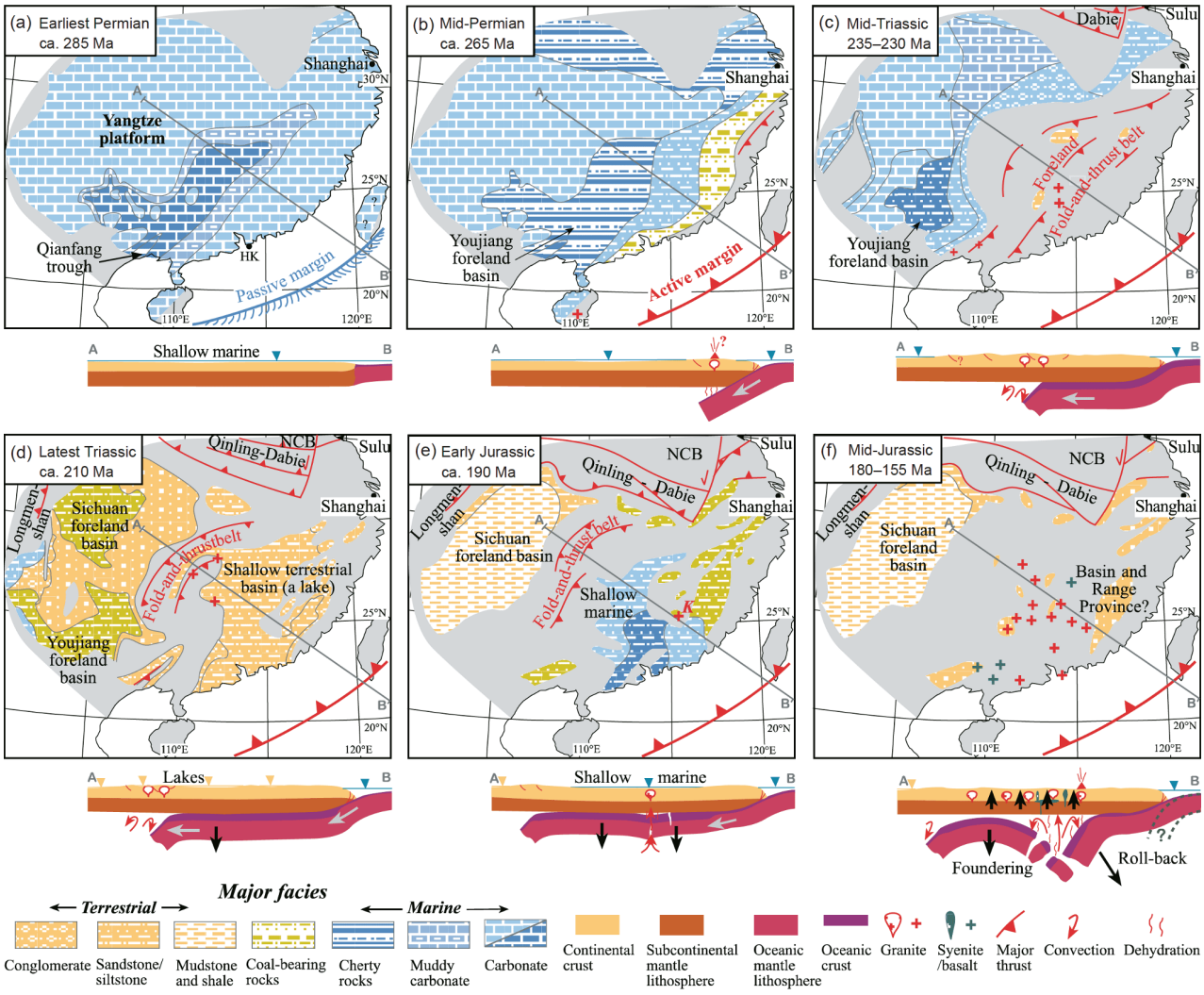

Figure 6 Orogenic evolution of South China fold belt during Permian-Jurassic time and flat subduction (Li and Li, 2007).

Zheng and Wu, 2009; Zhu et al., 2012). Jurassic magmatic rocks, consisting mainly of andesite, occur predominantly in the eastern part of the North China Craton (Figure 7a) and have an adakitic composition that indicates a relatively low-temperature magma (Wu et al., 2019). Early Cretaceous magmatism shows a wider distribution and different compositions to the Jurassic rocks. This spatial-temporal distribution of magmatism has been interpreted to reflect flat subduction during the Jurassic (Wu et al., 2019).

During the Early Jurassic (Figure 7b), normal subduction of the Pacific plate produced arc magmatism close to the trench. Flat subduction of the oceanic slab took place during the Late Jurassic (Figure 7c), due to the arrival of a relatively buoyant oceanic plateau at the subduction zone. Flat subduction was accompanied by lithospheric thickening and westward migration of the magmatic arc. During the Early Cretaceous (Figure 7d), the gravitationally unstable slab subducted deeper into the mantle, promoting a direct contact between the hot asthenospheric mantle and the root of the craton. This process was accompanied by asthenospheric- and lithospheric-derived magmatism, and resulted in lithospheric thinning. During the Late Cretaceous (Figure 7e), the lithosphere was further destroyed by crustal stratification, mechanical erosion, and hydration weakening. Accordingly, the thick cratonic lithospheric mantle was replaced by a new lithospheric mantle, giving rise to the formation of a broad plateau (North China Altiplano).

5. Formation mechanism of flat subduction

The formation mechanism of flat subduction is debated. Since van Hunen et al. (2000) first used numerical modeling to explore the formation mechanism of flat subduction, in the past 20 years, scholars have carried out much research and gained an essential understanding of the formation mechanism of the subduction. Major factors that affect the formation of flat subduction are: (1) the presence of an

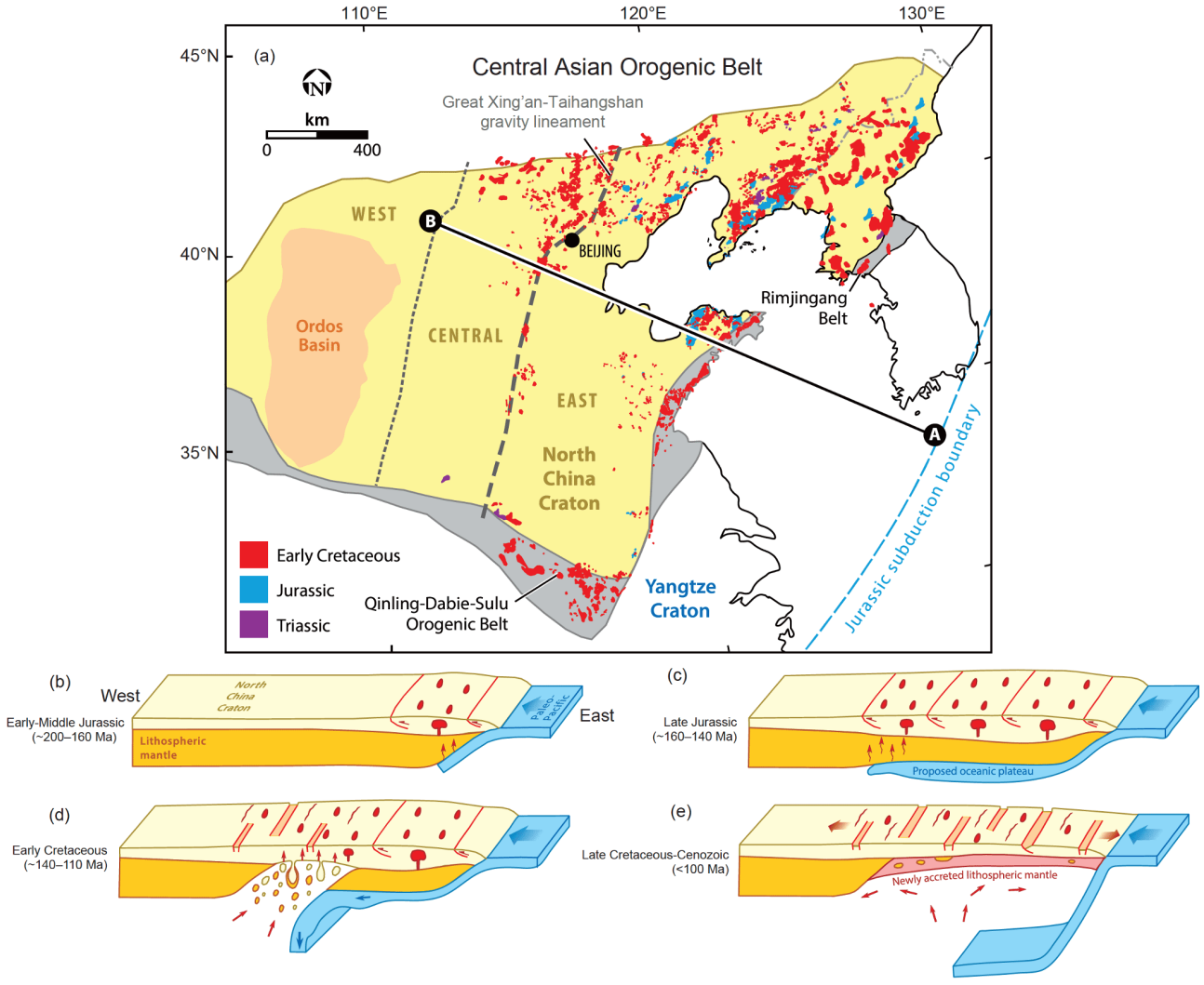

Figure 7 Schematic diagram of the flat subduction leading to the destruction of the North China Craton (modified after Wu et al., 2019). (a) The distribution of Mesozoic intrusive rocks in the North China Craton; (b)–(e) conceptual model of flat subduction leading to the destruction of the Late Mesozoic North China Craton.

anomalously buoyant material (e.g., oceanic plateau, oceanic ridge, or seamount chain) within the subducting plate (van Hunen et al., 2000, 2002a, 2004; Taramón et al., 2015; Hu et al., 2016; Liu and Currie, 2016; Axen et al., 2018); (2) overthrusting of the overriding plate (van Hunen et al., 2000, 2002b, 2004; Huangfu et al, 2016a; Liu and Currie, 2016); (3) hydrodynamic suction at the interface between the subducting and overriding plates (van Hunen et al., 2004; Manea et al., 2012; Rodríguez-González et al., 2012; Hu et al., 2016; Liu and Currie, 2016); and (4) trench retreat (Manea and Gurnis, 2007; Liu and Stegman, 2011; Manea et al., 2012). These mechanisms are discussed below, with insights from dynamic simulations.

5.1 Subduction of oceanic plateaus, oceanic ridges, and seamount chains

The formation of oceanic plateaus, oceanic ridges, and seamounts has been linked to the voluminous magmatism associated with large igneous provinces (Ben Avraham et al., 1981; Kerr, 2014). In these areas, the oceanic crust is anomalously thick (21–26 km) and is characterized by a low density of 2.79–2.84 kg m^{-3} (Tetreault and Buiter, 2014). Therefore, an oceanic lithosphere consisting of oceanic plateaus, oceanic ridges, and seamounts is anomalously buoyant. The effect of oceanic plateaus on the formation of flat subduction has been studied by van Hunen et al. (2002a) using two-dimensional finite-element numerical modeling. The authors considered an oceanic plateau (400 km across) with a crustal thickness of 18 km, simulating the Nazca Ridge (Figure 8). Their models also consider the transition from basalt to eclogite (van Hunen et al., 2002a), and yield the following results. (1) The ability of basalt to maintain a metastable state in the eclogite stability domain is a key factor in determining whether the oceanic plateau can maintain buoyancy for a long time; in other words, for flat

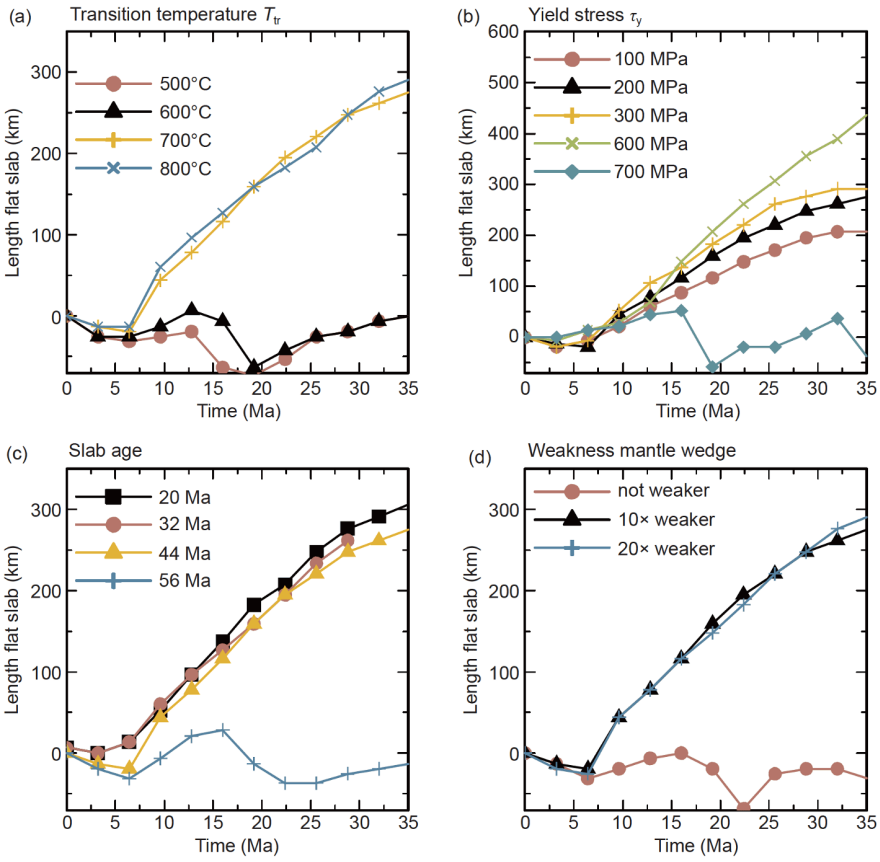

Figure 8 Relationship between flat subduction and key parameters (van Hunen et al., 2002a). (a) Transition temperature; (b) yield stress; (c) slab age; (d) relative strength of the mantle wedge.

subduction to form, the rate of phase transition must be sufficiently slow at temperatures of 600–700°C. (2) The maximum yield stress of the subducting slab cannot exceed 600 MPa; otherwise, flat subduction cannot occur. (3) Flat subduction is more likely to develop when the subducting oceanic lithosphere is relatively young. (4) The transition from steep to flat subduction requires weakening of the mantle wedge. (5) Finally, the length of the flat slab (in the direction of subduction) is less than 300 km if the flat subduction is driven by an oceanic plateau; the formation of larger flat slabs requires other mechanisms. The two-dimensional model of van Hunen et al. (2002a) did not consider the effects of dragging the surrounding plates parallel to the trench, which might offset the buoyancy of the oceanic plateau.

Three-dimensional physical simulations by Martinod et al. (2005) show that flat subduction is not produced if the linear oceanic ridge is oriented perpendicular to the trench. However, the presence of a buoyant oceanic anomaly parallel to the trench can lead to flat subduction. Other physical simulations by Espurt et al. (2008) further confirmed that specific conditions are required for the formation of flat subduction. For example, the oceanic plateau must be hundreds of kilometers in length to offset the negative buoyancy of the oceanic plate.

Gerya et al. (2009) have investigated the roles of plate dehydration, mantle wedge melting, and topographic development during subduction. These authors used a two-dimensional thermodynamic simulation method (I2VIS) to study relationships between oceanic plateau subduction and flat subduction. The models considered a 200 km wide oceanic ridge with a crustal thickness of 18 km, comparable to the Nazca Ridge (Figure 9). The results showed that: (1) subduction of a medium-scale oceanic plateau cannot cause significant slab flattening and weakening of magmatism; (2) The decrease of lithospheric mantle density in the subducting plate is conducive to the formation of flat subduction. In other words, the formation of flat subduction is mainly dependent on the state of the subducting plate; and (3) flat subduction leads to a dramatic decrease in magmatic activity, directly linked to the disappearance of the hot mantle wedge, but has nothing to do with the mechanism of forming flat subduction.

Based on the results of two-dimensional thermo-mechanical simulations, Axen et al. (2018) argued that the formation of the 1000-km-long Laramide orogeny required subduction of a very large (1000 km across) oceanic plateau (Shatsky Rise). The authors also pointed out that lithospheric mantle

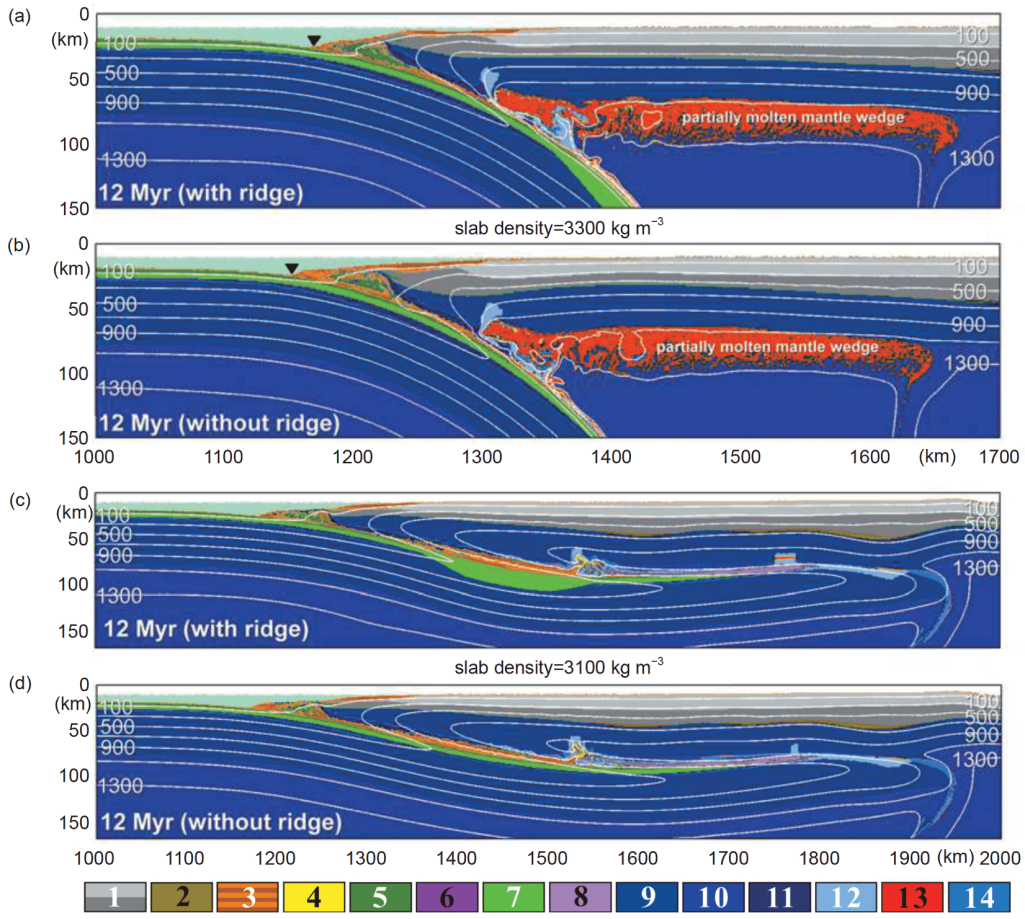

Figure 9 Model evolution results in 12 Myr (modified after Gerya et al., 2009). (a) and (b) Subducting oceanic mantle lithosphere density is 3300 kg m^{-3}; model a and b with and without a ridge, respectively. (c) and (d) Subducting oceanic mantle lithosphere density is 3100 kg m^{-3}; model (c) and (d) with and without a ridge, respectively. Mass melting occurs in (a) and (b) (red area). The solid white line represents the isotherm, the unit is °C. Color code: 1, 2: continental crust (1: solid, 2: partially molten); 3, 4: sediments (3: solid, 4: partially molten); 5, 6: upper (basaltic) oceanic crust (5: solid, 6: partially molten); 7, 8: lower (gabbroic) oceanic crust (7: solid, 8: partially molten); 9, 10: dry mantle (9: lithospheric, 10: asthenospheric); 11, 12, 13, 14: hydrated mantle (11: serpentinized, 12: serpentine-free, 13: partially molten, 14: quenched after melting).

serpentinite within the subducting slab can partially offset the negative buoyancy generated by eclogite. The presence of serpentinite also reduces the friction between the subducting and overriding plates (Reynard, 2013), thus further promoting flat subduction (Marot et al., 2014).

5.2 Overthrusting of the overriding plate

Another important factor affecting the formation of flat subduction is the movement of the overriding plate, which can affect the dip angle of the subducting plate (Cross and Pilger, 1978; Uyeda and Kanamori, 1979; Vlaar, 1983; Jarrard, 1986). In most present-day flat subduction zones, the overriding plate is moving towards the trench (Lallemand et al., 2005; Huangfu et al., 2016b). For example, the absolute velocity of the South American plate in the plated subduction zone of Chile, Peru, and Ecuador is 4.5, 4.5 and 3.8 cm a^{-1}, respectively; The absolute velocity of Cascadia in the West Coast of the United States is 2.4 cm a^{-1}. The effect of overriding-plate motion on flat subduction has been investigated by van Hunen et al. (2000) using two-dimensional finite-element numerical modelling. The authors found that the movement of the overriding plate towards the trench has a positive effect on the development of flat subduction. The important role of the overthrusting continent has been confirmed in a subsequent study (van Hunen et al., 2004).

The influence of plate velocity on subduction angle has been studied by Arcay et al. (2008) using thermochemical convection numerical modelling. These authors found that stationary or retreating overriding plates are characterized by backarc extension and a steep subduction angle. In contrast, an overriding plate that moves towards the trench promotes flattening of the slab dip angle. However, three-dimensional finite-element numerical modelling by Manea et al. (2012) found that movement of the overriding-plate alone is insufficient to explain the origin of the flat subduction segment in central Chile.

Relationships between absolute plate velocities and flat

subduction have been systematically analyzed by Huangfu et al. (2016b), using two-dimensional thermodynamic numerical modelling (I2VIS). The authors considered subduction of a 40 Ma oceanic slab. The results show that when the initial subduction angle is small, under the condition of low-speed ocean subduction ($\leq$3 cm a^{-1}), the smaller absolute thrust rate ($\geq$1 cm a^{-1}) can cause the flat subduction; for the middle and high-speed ocean subduction (>3 cm a^{-1}), the occurrence of flat subduction requires that the absolute thrust velocity of the overriding plate is not smaller than the absolute subduction velocity of the ocean plate. For an initial higher-angle subduction, a higher velocity of the overriding plate ($\geq$10 cm a^{-1}) and low rates of oceanic subduction are required to allow flat subduction. A higher initial subduction angle plays an important role in suppressing the formation of flat subduction segments. Finally, Huangfu et al. (2016b) concluded that higher rates of subduction can suppress the formation of flat subduction by overcoming the coupling force between the plates.

5.3 Hydrodynamic suction

During subduction, corner flow is developed in the asthenospheric wedge, in the area between the subducting plate and the overriding plate. This flow exerts an uplift force on the subducting slab (referred to as hydrodynamic suction), which can partially offset the negative buoyancy of the slab (Batchelor, 1967; Tovish et al., 1978). Therefore, hydrodynamic suction acts to reduce the slab dip angle, particularly if the original dip angle is relatively low, thus contributing to the development of flat subduction (Jischke, 1975; Stevenson and Turner, 1977; Tovish et al., 1978). Manea and Gurnis (2007) highlighted the importance of hydrodynamic suction in determining the slab geometry. They found that the negative pressure of the mantle wedge increases when the low-viscosity wedge is shallower, thereby resulting in a lower dip angle of the slab. Flat subduction occurs when the viscosity of the wedge is lower than that of the surrounding asthenosphere (Manea and Gurnis, 2007). Furthermore, the gradual closure of the mantle wedge hinders heat- and asthenosphere-convection, leading to a decrease in the slab dip angle (Arcay et al., 2008).

The presence of a thick cratonic root can also enhance the role of hydrodynamic suction. Results from numerical modelling have shown that hydrodynamic suction plays an important role if the overriding plate is excessively thick and cold, thus leading to flat subduction (Manea et al., 2012; Rodríguez-González et al., 2012). Rodríguez-González et al. (2012) have further suggested that the thermal state of the overriding plate has a larger effect on the slab dip angle than the age of the subducting lithosphere. Based on thermodynamic numerical models, Taramón et al. (2015) have shown that steep subduction occurs when the overriding plate is not composed of a cratonic lithosphere (Figure 10a). In the models, flat subduction was achieved when a craton was added to the overriding plate close to the trench (Figure 10b). When a craton design is added to the overriding slab away from the trench (Figure 10c), the results show a steep subduction, because the tension increases while the plate was subducting continuously, and the suction force of the plate is

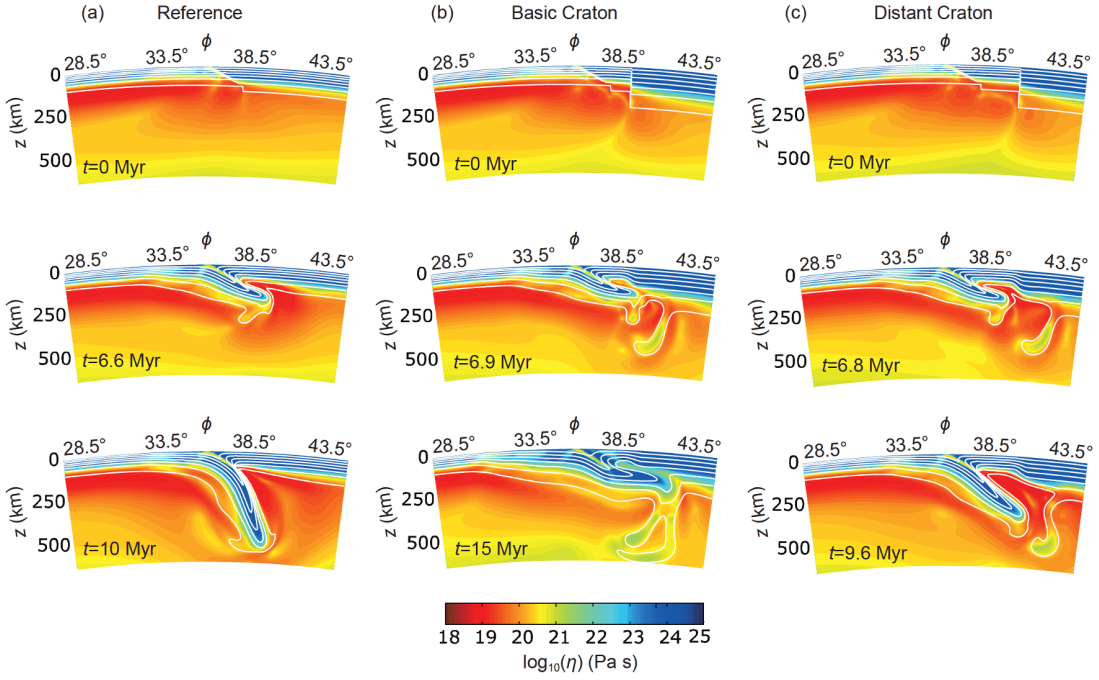

Figure 10 Model results of Taramón et al. (modified after Taramón et al., 2015). (a) Reference model without craton. (b) Based on the model (a), there is a craton at 3° from the trench. (c) Based on the model (a), there is a craton at 4° from the trench.

not enough to bend the plate to a horizontal state. The simulation results show that the craton creates a more favorable dynamic condition for the flat subduction of the buoyancy subduction plate. For example, in the case of the oceanic plateau subduction, the suction force of the craton can offset the eclogite of the crust, making it more common to see the oceanic plateau under the craton plate. Although the model c has no flat-slab effect, the subduction angle is smaller than the model a, further indicating that the hydrodynamic suction has the effect of reducing the subduction angle (Taramón et al., 2015). Antonijevic et al. (2015) also consider the hydrodynamic suction is one of the conditions for generating flat subduction. Liu and Currie (2016) used the two-dimensional SOPALE finite element program to study the dynamics of the Farallon plate, and also pointed out that the thick Colorado Plateau increases the suction between the plates to further reduce the subduction angle, therefore conducive to the flat subduction of the plates.

5.4 Trench retreat

Trench movement affects the structure of the subduction zone (Kincaid and Olson, 1987; Zhong and Gurnis, 1995; Christensen, 1996). Manea and Gurnis (2007) used two-dimensional numerical simulation experiment to study the relationship between the movement of the trench and the angle of the subduction, and found that the retreat of the trench would cause the change of the dip angle of the plate: When the subducting plate reaches the depth of about 100 km, the angle of the plate can be reduced to less than 15°. They believe that the trench retreat is a necessary condition for the formation of a plate dive. In the case of trench advance, the models by Manea and Gurnis (2007) did not develop flat subduction. We note, however, that these models were based on the assumption that the rate of trench retreat is equal to the velocity of the overriding plate (which is not always the case). The role of trench retreat in reducing the slab dip angle has also been shown by Liu and Stegman (2011), who used finite-element modelling (CitcomS) to simulate flat subduction of the Farallon plate. Antonijevic et al. (2015) based on the three-dimensional numerical simulation model of the shear wave velocity structure of the flat plate region in Peru, also pointed out that the trench retreat is one of the reasons for the plate flattening. Schepers et al. (2017) argued in the study of the formation mechanism of the Andean plate segment: the advancement of the South American plate forced the retreat of the Andean Trench, which is the driving force for the formation of the flat subduction. When the trench retreat is equal to the plate rotation, there is no plate subduction, and when the trench retreat is greater than the plate rotation, the flat subduction occurs.

Trench retreat should not be confused with overthrusting of the overriding plate. Trench retreat is an active process, which is commonly characterized by high plate velocities (e.g., Tonga area), which is conducive to the opening of the backarc basin and the formation of trench-arc-basin system. In contrast, overthrusting of the overriding plate is a passive process that is characterized by relatively low plate velocities (e.g., western South America) and is not responsible for the formation of a trench-arc-basin system. Trench retreat alone, while promoting slab flattening, is insufficient for the development of flat subduction. Western Pacific subduction zones, for example, are currently subjected to trench retreat, but are not associated with flat subduction. Recently, Schepers et al. (2017) explored the relationship between the retreat of the trench and the thrust velocity of the overriding plate. They found that the thrust of the overriding plate forced the trench to retreat as an important factor in the formation of flat subduction, but the thrust velocity of the overriding plate is not equal to the retreat speed of the trench. They are related to the rate and rotation of the subducting plate. Only when the trench retreat rate is greater than the plate rotation will the flat subduction occur.

5.5 Discussion

5.5.1 Relationships between factors that affect flat subduction

Factors that affect flat subduction include the subduction of oceanic plateaus, overthrusting of the overriding plate, hydrodynamic suction, and trench retreat. These factors may operate simultaneously and affect each other during the formation of flat subduction. In the following section, we discuss the relative importance of the various factors.

Oceanic plateaus and oceanic ridges occur throughout the Pacific Rim (Figure 2) and are generally considered to play a major role in the development of flat subduction (e.g., van Hunen et al., 2004). Conversely, based on numerical modelling results, some authors have suggested that the subduction of medium-scale oceanic plateaus is an insufficient factor for the development of flat subduction (e.g., Gerya et al., 2009). The relative buoyancy of an oceanic plateau is attributed to the thickened basaltic crust and the depleted underlying lithospheric mantle (Kerr, 2014). However, in the course of subduction, the relatively light basaltic oceanic crust is expected to change to eclogite, which is denser than the mantle (van Hunen et al., 2004). This means that after eclogitization, subducted oceanic plateaus cease to behave as buoyant anomalies that can drive flat subduction. To sustain buoyancy, it is possible that basalt remains metastable in the eclogite stability field (e.g., at temperatures of 400–800°C; Ahrens and Schubert, 1975; Rubie, 1990; Hacker, 1996). Numerical modeling results show that thickened oceanic crust can maintain buoyancy if phase transition occurs at temperatures higher than 600°C (van Hunen et al., 2002a). In such cases, flat subduction can be developed. Similar con-

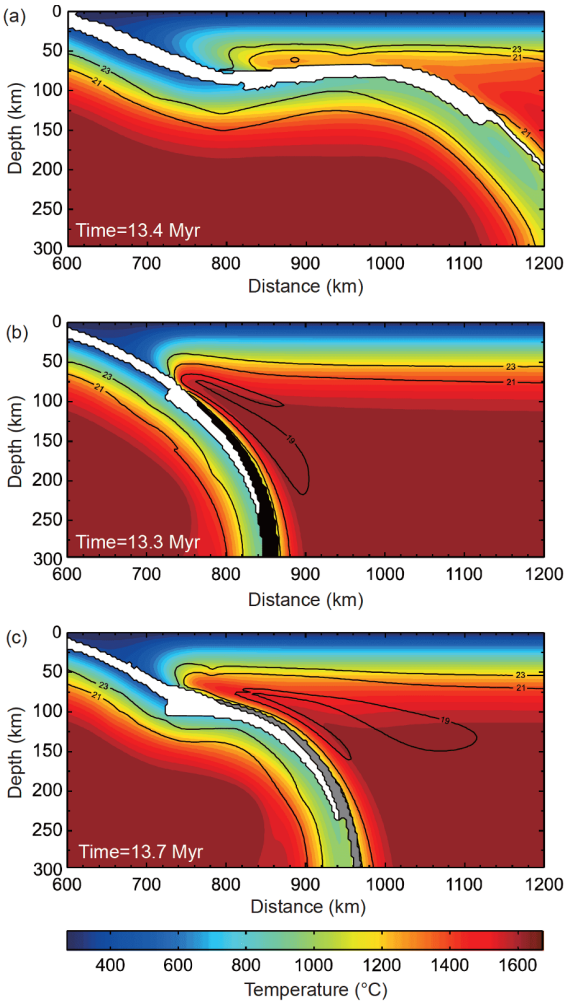

Figure 11 Relationship between flat subduction and eclogites (Arrial and Billen, 2013). (a) The oceanic crust has no eclogitization and a flat subduction occurs; (b) the oceanic crust is complete eclogitization and a steep subduction occurs; (c) the oceanic crust has partial eclogitization and a flat subduction occurs. White: basalt; Black: complete eclogitization; Gray: partial eclogitization. The solid black line is the isoviscosity line.

clusions have been drawn by Arrial and Billen (2013), who showed that flat subduction can be produced when the subducting oceanic crust is not subjected to complete eclogitization (Figure 11a and 11c). In cases of complete eclogitization, the slab dip angle remains steep (Figure 11b). Therefore, in the future study of the oceanic plateau buoyancy mechanism, we need to focus on the process of oceanic eclogite lithification.

Serpentinization of mantle peridotite is also an important factor, given that serpentine is ubiquitous in subducting oceanic crust and its density is relatively low (<2700 kg m^{-3}; Ranero et al., 2003; Grevemeyer et al., 2007; Lefeldt et al., 2012; Reynard, 2013). Therefore, the presence of serpentine in the subducting slab can offset the negative buoyancy generated by eclogite, while also controlling deformation and the volume of the oceanic crust (Angiboust and Agard, 2010). The presence of serpentine within the subducting oceanic plate has previously been considered to occur 1–2 km below the Moho (Ranero et al., 2003; Ranero and Sallarès, 2004), leading numerical modelers to incorporate a 1-km-thick serpentinite layer in their models (Gerya et al., 2009). Based on more recent seismic studies, it has been suggested that a major layer of serpentinite exist 4–5 km below the Moho (Contreras-Reyes et al., 2008; van Avendonk et al., 2011; Lefeldt et al., 2012), thus significantly increasing the positive buoyancy of the subducting slab. This important factor has not received much attention in previous studies that possibly underestimated the buoyancy of the subducting plate. The results of many numerical models indicate that the spatial extent of oceanic plateaus must be large to cause flat subduction (Martinod et al., 2005; Arrial and Billen, 2013; Betts et al., 2015). However, the subduction of many buoyant anomalies, such as the Emperor seamount chain, the Magellan seamount chain, and the Louisville oceanic plateau, did not seem to affect the slab geometry (Skinner and Clayton, 2013). The abnormal buoyancy of the oceanic plateau can promote the formation of flat subduction. Due to the complexity of the subduction zone, including: plate dehydration, material phase transformation, etc., the subducting plate's own buoyancy and the surrounding environment of the subduction zone are affected. This mechanism needs further confirmation.

Numerical simulations by van Hunen et al. (2004) showed that the overthrusting continent is considerably more important in promoting flat subduction than is an oceanic plateau. However, there are many examples were flat subduction is not developed regardless of the overriding plate moving towards the subduction zone (Schellart et al., 2008). In eastern Asia, the development of flat subduction segments since the late Mesozoic was likely controlled by buoyant anomalies (Li and Li, 2007; Wu et al., 2019), given that overthrusting of the overriding plate is not apparent from plate reconstructions (Yang et al., 2019). The movement of the overridingplate towards the trench is unable to flatten steep slabs (Manea et al., 2012) unless the overriding plate is very thick (>200 km) or the rate of trench retreat is very high (>4 cm yr^{-1}) (van Hunen et al., 2000; Cizkova et al., 2002). The numerical simulation results of Manea et al. (2012) show that the overriding plate movement of the normal thickness lithosphere and the retreat of the trench are not sufficient to explain the Chilean slab. Only the combination of the movement of the thick craton lithosphere and the trench retreat can reproduce the spatiotemporal evolution of the slab attenuation and its associated upper plate deformation and volcanism. The thickness of the overriding plate can cause the physical mechanism of the plate to be reduced by the pressure in the mantle wedge caused by flow (Stevenson and Turner, 1977). The narrowing of the mantle wedge or decreasing the wedge viscosity will increase the negative pressure and pull the plate upwards to bend it, and the sub-

duction angle becomes smaller (van Hunen et al., 2004). Ultimately, it is difficult to form a flat subduction by a single overthrusting continent, but with other mechanisms, such as: oceanic plateau, trench retreat or increased hydrodynamic suction, and then can form a flat subduction (Figure 12a).

Three-dimensional dynamic modelling by Hu et al. (2016) showed that the age of the oceanic plate, the presence of an oceanic plateau, and hydrodynamic suction have all contributed to the development of flat subduction segments in South America. The thick overriding plate increases the hydrodynamic suction and thus reduces the subduction angle, while thick cratonic roots further lead to a smaller subduction angle, and the addition of the oceanic plateau or aseismic ridges flattens the young subducting plate, which in turn produces a flat subduction. The results showed that buoyancy characteristics (ocean plateau, oceanic ridge or seamount chain) contribute significantly to the formation of flat subduction in Peru and Chile; at the same time, it also emphasizes that although buoyancy can effectively decrease the plate angle, it is necessary to add other mechanisms (e.g., hydrodynamic suction, etc.) to be able to predict a larger flat subduction.

The relative contributions of factors that control flat subduction have been explored by Liu and Currie (2016) using two-dimensional dynamic models, with an emphasis on the presence of the thick lithosphere beneath the Colorado Plateau. These authors found that all three factors (overriding plates' motion, hydrodynamic suction generated by the presence of the thick Colorado Plateau lithosphere, and the oceanic plateau) can lead to the decrease of the angle of the plate with time. Among them, the influence of the trenchward continental motion is the largest. As the speed of the continent increases, the angle of the plate decreases gradually. However, in order to induce flat subduction of an old oceanic plate, multiple factors are required. First, trenchward continental motion causes slab dip to decrease. Once a low-angle subduction zone forms, the transition to a sub-horizontal geometry requires: (1) subduction of a low-density oceanic plateau, and (2) a breakoff event that removes the dense frontal slab. In addition, the model indicates that the flat subduction does not depend on the Colorado Plateau, but its lithospheric thickness controls the depth of the flat slab. This result further emphasizes the mutual promotion and close relationship between the mechanisms during the formation of the flat subduction.

In summary, buoyancy, overthrusting continent, hydro-

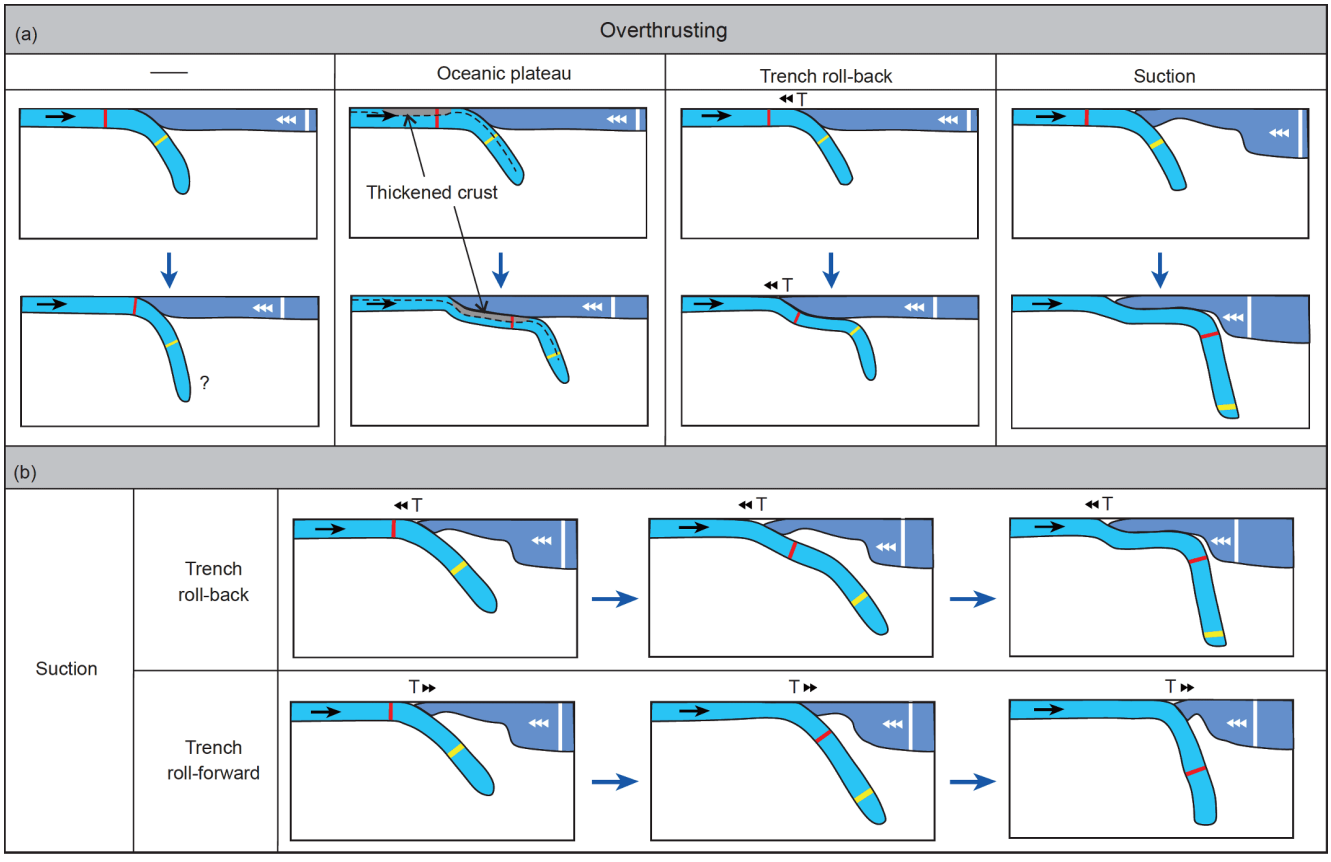

Figure 12 The relationship between the various factors that form the plate subduction. (a) The relationship between the overthrusting plate and the oceanic plateau, trench retreat and hydrodynamic suction; (b) the relationship between hydrodynamic suction and trench movement. Modified after Manea et al. (2012) and Liu and Currie (2016).

dynamic suction and trench retreat are all conducive to the formation of flat subduction, but there is no uniform factor as the formation mechanism of the current flat subduction area. It is difficult to distinguish between these factors based on geological or geophysical observations. Flat subduction as an uncommon subduction pattern may be controlled by multiple factors. The origin of flat subduction in a particular area requires a specific analysis and cannot be generalized. For example, the development of flat subduction in South America seems to correspond to the presence of oceanic ridges and the westward movement of the South American continent, whereas the subduction of an oceanic ridge in other areas is not associated with flat subduction.

The presence of oceanic plateaus and the size of the buoyant anomalies influence the development of flat subduction. Overthrusting of the overriding plate also plays a crucial role in the formation of flat subduction, which can further be promoted by hydrodynamic suction and trench retreat. Trench advance does not seem to contribute to the formation of flat subduction (Figure 12b). In the flat subduction mechanism, the overthrusting and the oceanic plateau are the key factors, the hydrodynamic suction comes as the secondary factor, and the trench retreat is a necessary condition for the formation of flat subduction. Increasing the hydrodynamic suction and trench retreat is more likely to form a flat subduction, and also increase the length of the flat subduction.

5.5.2 Model limitations and suggestions for future modelling

Since the physical parameters inside the Earth cannot be directly measured and cannot observe the ongoing process, we can only rely on indirect measurements such as geological observations, geochemical characteristics of volcanic activities, and geophysical tools such as tomography. Geological and geophysical observations can only provide limited information on Earth dynamics, but numerical modeling is an effective tool for simulating dynamic processes. Accordingly, numerical simulations play a vital role in the study of flat subduction. However, the results are commonly biased by the design of a simplified model. For example, the results can be biased by the age of the oceanic crust, the abrupt change in the thickness of the overriding plate, the size of the buoyant anomalies, the shape of the subduction zone (i.e. concave, convex, or straight), and the angle of the subduction direction relative to the trench.

At the same time, due to the extremely complex internal structure of the Earth, numerical modeling can't completely restore its parameters, so simplified means are used, which may produce certain errors. Previous numerical models of flat subduction have focused on the development of the flat slab, but have not considered the subsequent evolution of the slab. As a result, they are more of conceptual models or speculations. On the one hand, the numerical modeling results generally show that after the flat subduction occurs, the front plate is broken, and the front plate is not dragged, which is not conducive to the rollback of the subducting plate. On the other hand, the current numerical model of flat subduction has less consideration of rock phase transition, and does not fully consider the negative buoyancy generated by rock phase transition, so it is difficult to let the flat subduction self-consistency to disassembled or destroy. These two aspects should be taken more care of for the future research on the flat subduction.

In addition, because of the irreversibility of mantle convection, we cannot easily reverse the previous state from existing data. Since the accompanying data assimilation method has been widely used in atmospheric and marine scientific research. Liu and Gurnis (2010) introduced it to the geoscience research field and illustrated systematically the application of such method in geosciences and its geophysical significance. Liu and Gurnis (2010) use the accompanying data assimilation method to invert the flat subduction process of the Late Cretaceous Farallon plate under the North American plate. The flat subduction resulted in large-scale dynamic subsidence and seawater intrusion in the western North American continent, thus explained the West Inner Sea of North American that has been forming almost throughout the Late Cretaceous time. As the accompanying data assimilation method can invert an irreversible physical process, it has broad application prospects in solid geophysical research. It is not only suitable for large-scale mantle convection, but also for medium- and small-scale earth continuum motion.

Therefore, considering the actual geological and boundary conditions, using the accompanying data assimilation method (Liu and Gurnis, 2010), and carrying out three-dimensional high-resolution thermo-mechanical numerical simulation research to explore the formation mechanism of flat subduction and to quantify the proportion of various mechanisms is the key direction and means of future research.

6. Conclusions

We systematically analyzed and summarized previous results on the origin of flat subduction and its geological effects. A particular emphasis was given to numerical simulations. The following three conclusions are drawn.

(1) During flat subduction, coupling between the upper and lower plates significantly cools the thermal structure of the overriding plate, thus reducing the surface heat flow and triggering large intermediate and deep earthquakes. Intracontinental surface shows special geological phenomena during flat subduction: The deformation of the overriding plate migrates to the intracontinent; Island arc magma ac-

tivity migrates, weakens or disappears into the intracontinent. These characteristics are an important geological basis for judging or speculating the flat subduction. In addition, the adakite produced by the melting of the flat-slab oceanic crust is closely related to large and giant ore deposits.

(2) Factors controlling the development of flat subduction include buoyant anomalies within the subducting plate (e.g., oceanic plateaus, oceanic ridges, and seamount chains), overthrusting of the overriding plate, trench retreat, and hydrodynamic suction. The most crucial factors are the overthrusting of the overriding plate and the presence of oceanic plateaus. Hydrodynamic suction contributes to lowering the slab dip angle, but is insufficient to form flat subduction. Trench retreat is necessary for the formation of flat subduction. Hydrodynamic suction and trench retreat promote flat subduction and increase the length of the flat slab segment.

(3) Flat subduction is a three-dimensional dynamic process. Previous attempts to model this process in two dimensions have limited implications because they did not take into account along-strike variations in the subduction zone and the impacts of surrounding plates on the subduction process. In addition, previous numerical experiments have not fully considered the effects of magmatism, eclogitization, and serpentinization. Future attempts to understand flat subduction should use the accompanying data assimilation method, and combine geological and geophysical observations with three-dimensional high-resolution thermo-mechanical modeling that considers the effects of crustal eclogitization (negative buoyancy) and mantle serpentinization (positive buoyancy).

Acknowledgements *We thank professors Yi CHEN and Bo WAN for their constructive comments. We also thank the reviewers for providing constructive comments that substantially improved the manuscript. This work was supported by the National Key Research and Development of China (Grant No. 2016YFC0600406), the National Natural Science Foundation of China (Grant Nos. 41731072, 41574095), and the Strategic Priority Research Program (B) of the Chinese Academy of Sciences (Grant No. XDB18000000).*

References

Abbott D, Drury R, Smith W H F. 1994. Flat to steep transition in subduction style. Geology, 22: 937–940
Ahrens T J, Schubert G. 1975. Gabbro-eclogite reaction rate and its geophysical significance. Rev Geophys, 13: 383–400
Angiboust S, Agard P. 2010. Initial water budget: The key to detaching large volumes of eclogitized oceanic crust along the subduction channel? Lithos, 120: 453–474
Antonijevic S K, Wagner L S, Kumar A, Beck S L, Long M D, Zandt G, Tavera H, Condori C. 2015. The role of ridges in the formation and longevity of flat slabs. Nature, 524: 212–215
Arcay D, Lallemand S, Doin M P. 2008. Back-arc strain in subduction zones: Statistical observations versus numerical modeling. Geochem Geophys Geosyst, 9: Q05015
Arrial P A, Billen M I. 2013. Influence of geometry and eclogitization on oceanic plateau subduction. Earth Planet Sci Lett, 363: 34–43
Axen G J, van Wijk J W, Currie C A. 2018. Basal continental mantle lithosphere displaced by flat-slab subduction. Nat Geosci, 11: 961–964
Barazangi M, Isacks B L. 1976. Spatial distribution of earthquakes and subduction of the Nazca plate beneath South America. Geology, 4: 686–692
Batchelor G K. 1967. An Introduction to Fluid Dynamics. Cambridge, U K: Cambridge University Press
Beate B, Monzier M, Spikings R, Cotten J, Silva J, Bourdon E, Eissen J P. 2001. Mio-Pliocene adakite generation related to flat subduction in southern Ecuador: The Quimsacocha volcanic center. Earth Planet Sci Lett, 192: 561–570
Ben-Avraham Z, Nur A, Jones D, Cox A. 1981. Continental accretion: From oceanic plateaus to allochthonous terranes. Science, 213: 47–54
Betts P G, Moresi L, Miller M S, Willis D. 2015. Geodynamics of oceanic plateau and plume head accretion and their role in Phanerozoic orogenic systems of China. Geosci Front, 6: 49–59
Bird P. 1988. Formation of the Rocky Mountains, Western United States: A continuum computer model. Science, 239: 1501–1507
Bourdon E, Eissen J P, Gutscher M A, Monzier M, Hall M L, Cotten J. 2003. Magmatic response to early aseismic ridge subduction: The Ecuadorian margin case (South America). Earth Planet Sci Lett, 205: 123–138
Cao M J, Qin K Z, Li J L. 2011. Research progress on the flat subduction and its metallogenic effect, two cases analysis and some prospects. Acta Petrol Sin, 27: 3727–3748
Chen S F, Wilson C J L. 1996. Emplacement of the Longmen Shan Thrust —Nappe Belt along the eastern margin of the Tibetan Plateau. J Struct Geol, 18: 413–430
Christensen U R. 1996. The influence of trench migration on slab penetration into the lower mantle. Earth Planet Sci Lett, 140: 27–39
Cizkova H, van Hunen J, van den Berg A P, Vlaar N J. 2002. The influence of rheological weakening and yield stress on the interaction of slabs with the 670 km discontinuity. Earth Planet Sci Lett, 193: 447–457
Cloos M, Shreve R L. 1996. Shear-zone thickness and the seismicity of Chilean- and Marianas-type subduction zones. Geology, 24: 107–110
Cole R B, Nelson S W, Layer P W, Oswald P J. 2006. Eocene volcanism above a depleted mantle slab window in southern Alaska. Geol Soc Am Bull, 118: 140–158
Conrad C P, Bilek S, Lithgow-Bertelloni C. 2004. Great earthquakes and slab pull: Interaction between seismic coupling and plate-slab coupling. Earth Planet Sci Lett, 218: 109–122
Contreras-Reyes E, Grevemeyer I, Flueh E R, Reichert C. 2008. Upper lithospheric structure of the subduction zone offshore of southern Arauco peninsula, Chile, at ~38°S. J Geophys Res, 113: B07303
Cross T A, Pilger R H. 1978. Tectonic controls of late cretaceous sedimentation, western interior, USA. Nature, 274: 653–657
Cui S Q, Li J R. 1983. On the circum-Pacific Indosinian movement in China (in Chinese). Acta Geol Sin, 57: 51–62
Davies J H. 1999. Simple analytic model for subduction zone thermal structure. Geophys J Int, 139: 823–828
Defant M J, Jackson T E, Drummond M S, De Boer J Z, Bellon H, Feigenson M D, Maury R C, Stewart R H. 1992. The geochemistry of young volcanism throughout western Panama and southeastern Costa Rica: An overview. J Geol Soc, 149: 569–579
Defant M J, Drummond M S. 1990. Derivation of some modern arc magmas by melting of young subducted lithosphere. Nature, 347: 662–665
Defant M J, Drummond M S. 1993. Mount St. Helens: Potential example of the partial melting of the subducted lithosphere in a volcanic arc. Geology, 21: 547–550
Deng J F, Mo X X, Zhao H L, Luo Z H, Du Y S. 1994. Lithosphere root /de-roting and activation of the east China continent (in Chinese with English abstract). Geosciences, 3: 349–356
Dickinson W R, Snyder W S. 1978. Plate tectonics of the Laramide orogeny. Geol Soc Am Mem, 151: 355–366

Dumitru T A, Gans P B, Foster D A, Miller E L. 1991. Refrigeration of the western Cordilleran lithosphere during Laramide shallow-angle subduction. Geology, 19: 1145–1148
English J M, Johnston S T. 2004. The laramide orogeny: What were the driving forces? Int Geol Rev, 46: 833–838
Espurt N, Funiciello F, Martinod J, Guillaume B, Regard V, Faccenna C, Brusset S. 2008. Flat subduction dynamics and deformation of the South American plate: Insights from analog modeling. Tectonics, 27: TC3011
Fromm R, Zandt G, Beck S L. 2004. Crustal thickness beneath the Andes and Sierras Pampeanas at 30°S inferred from Pn apparent phase velocities. Geophys Res Lett, 31: L06625
Fuis G S, Moore T E, Plafker G, Brocher T M, Fisher M A, Mooney W D, Nokleberg W J, Page R A, Beaudoin B C, Christensen N I, Levander A R, Lutter W J, Saltus R W, Ruppert N A. 2008. Trans-Alaska Crustal Transect and continental evolution involving subduction underplating and synchronous foreland thrusting. Geology, 36: 267–270
Gao S, Zhang B R, Jin Z M, Kern H, Ting-Chuan Luo H, Zhao Z D. 1998. How mafic is the lower continental crust? Earth Planet Sci Lett, 106: 101–117
Gardner T W, Fisher D M, Morell K D, Cupper M L. 2013. Upper-plate deformation in response to flat slab subduction inboard of the aseismic Cocos Ridge, Osa Peninsula, Costa Rica. Lithosphere, 5: 247–264
Gerya T V, Fossati D, Cantieni C, Seward D. 2009. Dynamic effects of aseismic ridge subduction: Numerical modelling. Eur J Mineral, 21: 649–661
Gerya T V, Yuen D A. 2003. Characteristics-based marker-in-cell method with conservative finite-differences schemes for modeling geological flows with strongly variable transport properties. Phys Earth Planet Inter, 140: 293–318
Gómez-Tuena A, LaGatta A B, Langmuir C H, Goldstein S L, Ortega-Gutiérrez F, Carrasco-Núñez G. 2003. Temporal control of subduction magmatism in the eastern Trans-Mexican Volcanic Belt: Mantle sources, slab contributions, and crustal contamination. Geochem Geophys Geosyst, 4: 8912
Grafe K, Frisch W, Villa I M, Meschede M. 2002. Geodynamic evolution of southern Costa Rica related to low-angle subduction of the Cocos Ridge: Constraints from thermochronology. Tectonophysics, 348: 187–204
Grevemeyer I, Ranero C R, Flueh E R, Kläschen D, Bialas J. 2007. Passive and active seismological study of bending-related faulting and mantle serpentinization at the Middle America trench. Earth Planet Sci Lett, 258: 528–542
Griffin W, Andi Z, O'reilly S, Ryan C. 1998. Phanerozoic evolution of the lithosphere beneath the Sino-Korean craton. In: Flower M F J, Chung S L, Lo C H, Lee T Y, eds. Mantle Dynamics and Plate Interactions in East Asia. Am Geophys Union, 27: 107–126
Grove T L, Till C B, Krawczynski M J. 2012. The role of H_2O in subduction zone magmatism. Annu Rev Earth Planet Sci, 40: 413–439
Gutscher M A. 2002. Andean subduction styles and their effect on thermal structure and interplate coupling. J South Am Earth Sci, 15: 3–10
Gutscher M A. 2018. Scraped by flat-slab subduction. Nat Geosci, 11: 889–893
Gutscher M A, Maury R, Eissen J P, Bourdon E. 2000a. Can slab melting be caused by flat subduction? Geology, 28: 535–538
Gutscher M A, Spakman W, Bijwaard H, Engdahl E R. 2000b. Geodynamics of flat subduction: Seismicity and tomographic constraints from the Andean margin. Tectonics, 19: 814–833
Hacker B R. 1996. Eclogite formation and the rheology, buoyancy, seismicity, and H_2O content of oceanic crust. Geophys Monogr Ser, 96: 337–346
Henderson L J, Gordon R G, Engebretson D C. 1984. Mesozoic aseismic ridges on the Farallon plate and southward migration of shallow subduction during the Laramide orogeny. Tectonics, 3: 121–132
Henry S G, Pollack H N. 1988. Terrestrial heat flow above the Andean subduction zone in Bolivia and Peru. J Geophys Res, 93: 15153–15162
Hsü K J, Li J, Chen H, Wang Q, Sun S, Şengör A M C. 1990. Tectonics of South China: Key to understanding West Pacific geology. Tectonophysics, 183: 9–39
Hu J, Liu L, Hermosillo A, Zhou Q. 2016. Simulation of late Cenozoic South American flat-slab subduction using geodynamic models with data assimilation. Earth Planet Sci Lett, 438: 1–13
Huangfu P P, Wang Y, Cawood P A, Li Z H, Fan W, Gerya T V. 2016a. Thermo-mechanical controls of flat subduction: Insights from numerical modeling. Gondwana Res, 40: 170–183
Huangfu P P, Wang Y, Fan W, Li Z, Wang Y, Zhou Y. 2016b. Numerical modeling of flat subduction: Constraints from the ocean-continent convergence velocity. Geotect Metal, 40: 429–445
Jarrard R D. 1986. Relations among subduction parameters. Rev Geophys, 24: 217–284
Jischke M C. 1975. On the dynamics of descending lithospheric plates and slip zones. J Geophys Res, 80: 4809–4813
Johnston S T, Thorkelson D J. 1997. Cocos-Nazca slab window beneath Central America. Earth Planet Sci Lett, 146: 465–474
Kay S M, Abbruzzi J M. 1996. Magmatic evidence for Neogene lithospheric evolution of the central Andean "flat-slab" between 30°S and 32°S. Tectonophysics, 259: 15–28
Kay S M, Mpodozis C. 2002. Magmatism as a probe to the Neogene shallowing of the Nazca plate beneath the modern Chilean flat-slab. J South Am Earth Sci, 15: 39–57
Kelemen P B, Hanghoj K. 2003. One view of the geochemistry of subduction-related magmatic arcs, with an emphasis on primitive andesite and lower crust. In: Rudnick R L, ed. Treatise in Geochemistry: The Crust. Oxford: Elsevier. 593–659
Kerr A C. 2014. Oceanic plateaus. In: Holland H D, Turekian K K, eds. Treatise on Geochemistry. Vol. 4: The crust. 2nd ed, Amsterdam: Elsevier. 631–667
Kincaid C, Olson P. 1987. An experimental study of subduction and slab migration. J Geophys Res, 92: 13832–13840
Lallemand S, Heuret A, Boutelier D. 2005. On the relationships between slab dip, back-arc stress, upper plate absolute motion, and crustal nature in subduction zones. Geochem Geophys Geosyst, 6: Q09006
Lefeldt M, Ranero C R, Grevemeyer I. 2012. Seismic evidence of tectonic control on the depth of water influx into incoming oceanic plates at subduction trenches. Geochem Geophys Geosyst, 13: Q05013
Leng W, Huang L. 2018. Progress in numerical modeling of subducting plate dynamics. Sci China Earth Sci, 61: 1761–1774
Li Z X. 1998. Tectonic evolution of the major East Asian lithospheric block since the Mid-Proterozoic: A synthesis. In: Martin F J, Chung S L, Lo C H, Lee T Y, eds. Mantle Dynamics and Plate Interactions in East Asia. Washington D C: Am Geophys Union Geodynamics Ser. 221–243
Li X H, Li Z X, Li W X, Wang Y. 2006. Initiation of the indosinian orogeny in South China: Evidence for a Permian magmatic arc on Hainan Island. J Geol, 114: 341–353
Li Z X, Li X H. 2007. Formation of the 1300-km-wide intracontinental orogen and postorogenic magmatic province in Mesozoic South China: A flat-slab subduction model. Geology, 35: 179–182
Liu L, Spasojevic S, Gurnis M. 2008. Reconstructing farallon plate subduction beneath North America back to the Late Cretaceous. Science, 322: 934–938
Liu L, Gurnis M. 2010. Dynamic subsidence and uplift of the Colorado Plateau. Geology, 38: 663–666
Liu L, Gurnis M, Seton M, Saleeby J, Müller R D, Jackson J M. 2010. The role of oceanic plateau subduction in the Laramide orogeny. Nat Geosci, 3: 353–357
Liu L, Stegman D R. 2011. Segmentation of the Farallon slab. Earth Planet Sci Lett, 311: 1–10
Liu S, Currie C A. 2016. Farallon plate dynamics prior to the Laramide orogeny: Numerical models of flat subduction. Tectonophysics, 666: 33–47
Livaccari R F, Burke K, Şengör A M C. 1981. Was the Laramide orogeny related to subduction of an oceanic plateau? Nature, 289: 276–278
Luyendyk B P. 1970. Dips of downgoing lithospheric plates beneath island arcs. Geol Soc Am Bull, 81: 3411–3416

Ma Y, Clayton R W. 2014. The crust and uppermost mantle structure of Southern Peru from ambient noise and earthquake surface wave analysis. Earth Planet Sci Lett, 395: 61–70
Manea V, Gurnis M. 2007. Subduction zone evolution and low viscosity wedges and channels. Earth Planet Sci Lett, 264: 22–45
Manea V C, Manea M. 2011. Flat-slab thermal structure and evolution beneath Central Mexico. Pure Appl Geophys, 168: 1475–1487
Manea V C, Pérez-Gussinyé M, Manea M. 2012. Chilean flat slab subduction controlled by overriding plate thickness and trench rollback. Geology, 40: 35–38
Manea V C, Manea M, Ferrari L, Orozco-Esquivel T, Valenzuela R W, Husker A, Kostoglodov V. 2017. A review of the geodynamic evolution of flat slab subduction in Mexico, Peru, and Chile. Tectonophysics, 695: 27–52
Marot M, Monfret T, Pardo M, Ranalli G, Nolet G. 2013. A double seismic zone in the subducting Juan Fernandez Ridge of the Nazca Plate (32°S), central Chile. J Geophys Res-Solid Earth, 118: 3462–3475
Marot M, Monfret T, Gerbault M, Nolet G, Ranalli G, Pardo M. 2014. Flat versus normal subduction zones: A comparison based on 3-D regional traveltime tomography and petrological modelling of central Chile and western Argentina (29°–35°S). Geophys J Int, 199: 1633–1654
Marshall J S, Anderson R S. 1995. Quaternary uplift and seismic cycle deformation, Península de Nicoya, Costa Rica. Geol Soc Am Bull, 107: 463–473
Martinod J, Funiciello F, Faccenna C, Labanieh S, Regard V. 2005. Dynamical effects of subducting ridges: Insights from 3-D laboratory models. Geophys J Int, 163: 1137–1150
Maxson J, Tikoff B. 1996. Hit-and-run collision model for the Laramide orogeny, western United States. Geology, 24: 968–972
Megard F, Philip H. 1976. Plio-Quaternary tectono-magmatic zonation and plate tectonics in the Central Andes. Earth Planet Sci Lett, 33: 231–238
Menzies M A, Fan W, Zhang M. 1993. Palaeozoic and Cenozoic lithoprobes and the loss of >120 km of Archaean lithosphere, Sino-Korean craton, China. Geol Soc Lond Spec Publ, 76: 71–81
Michaud F, Witt C, Royer J Y. 2009. Influence of the subduction of the Carnegie volcanic ridge on Ecuadorian geology: Reality and fiction. Geol Soc Am Mem, 204: 217–228
Mori L, Gómez-Tuena A, Cai Y, Goldstein S L. 2007. Effects of prolonged flat subduction on the Miocene magmatic record of the central Trans-Mexican Volcanic Belt. Chem Geol, 244: 452–473
Morris P A. 1995. Slab melting as an explanation of quaternary volcanism and aseismicity in southwest Japan. Geology, 23: 395–398
Muñoz M. 2005. No flat Wadati-Benioff Zone in the central and southern central Andes. Tectonophysics, 395: 41–65
Murphy J B, Oppliger G L, Brimhall G H, Hynes A. 1998. Plume-modified orogeny: An example from the western United States. Geology, 26: 731–734
Murphy J B, van Staal C R, Duncan Keppie J. 1999. Middle to late Paleozoic Acadian orogeny in the northern Appalachians: A Laramide-style plume-modified orogeny? Geology, 27: 653–656
Murphy J B, Hynes A J, Johnston S T, Keppie J D. 2003. Reconstructing the ancestral Yellowstone plume from accreted seamounts and its relationship to flat-slab subduction. Tectonophysics, 365: 185–194
Oldow J S, Bally A W, Avé Lallemant H G. 1990. Transpression, orogenic float, and lithospheric balance. Geology, 18: 991–994
Oleskevich D A, Hyndman R D, Wang K. 1999. The updip and downdip limits to great subduction earthquakes: Thermal and structural models of Cascadia, south Alaska, SW Japan, and Chile. J Geophys Res, 104: 14965–14991
Oyarzun R, Márquez A, Lillo J, López I, Rivera S. 2001. Giant versus small porphyry copper deposits of Cenozoic age in northern Chile: Adakitic versus normal calc-alkaline magmatism. Min Dep, 36: 794–798
Page R A, Stephens C D, Lahr J C. 1989. Seismicity of the Wrangell and Aleutian Wadati-Benioff Zones and the North American Plate along the Trans-Alaska Crustal Transect, Chugach Mountains and Copper River Basin, southern Alaska. J Geophys Res, 94: 16059–16082
Peacock S M, Rushmer T, Thompson A B. 1994. Partial melting of subducting oceanic crust. Earth Planet Sci Lett, 121: 227–244
Peacock S M. 1996. Thermal and petrologic structure of subduction zones. In: Bebout E, Schol D W, Kirby S H, Blatt J P, eds. Subduction: Top to Bottom. Geophys Monograph Ser, 96: 119–133
Penniston-Dorland S C, Kohn M J, Manning C E. 2015. The global range of subduction zone thermal structures from exhumed blueschists and eclogites: Rocks are hotter than models. Earth Planet Sci Lett, 428: 243–254
Price R A. 1981. The Cordilleran foreland thrust and fold belt in the southern Canadian Rocky Mountains. Geol Soc Lond Spec Publ, 9: 427–448
Protti M, Gu¨ndel F, McNally K. 1994. The geometry of the Wadati-Benioff zone under southern Central America and its tectonic significance: Results from a high-resolution local seismographic network. Phys Earth Planet Inter, 84: 271–287
Ramos V A, Folguera A. 2009. Andean flat-slab subduction through time. Geol Soc Lond Spec Publ, 327: 31–54
Ranero C R, Phipps Morgan J, McIntosh K, Reichert C. 2003. Bending-related faulting and mantle serpentinization at the Middle America trench. Nature, 425: 367–373
Ranero C R, Sallarès V. 2004. Geophysical evidence for hydration of the crust and mantle of the Nazca plate during bending at the north Chile trench. Geology, 32: 549–552
Reynard B. 2013. Serpentine in active subduction zones. Lithos, 178: 171–185
Rodgers J. 1987. Chains of basement uplifts within cratons marginal to orogenic belts. Am J Sci, 287: 661–692
Rodríguez-González J, Negredo A M, Billen M I. 2012. The role of the overriding plate thermal state on slab dip variability and on the occurrence of flat subduction. Geochem Geophys Geosyst, 13: Q01002
Rubie D C. 1990. Role of kinetics in the formation and preservation of eclogites. In: Carswell D A, ed. Eclogite Facies Rocks. New York: Chapman and Hall Press. 111–140
Sacks I S. 1983. The subduction of young lithosphere. J Geophys Res, 88: 3355–3366
Schellart W P, Stegman D R, Freeman J. 2008. Global trench migration velocities and slab migration induced upper mantle volume fluxes: Constraints to find an Earth reference frame based on minimizing viscous dissipation. Earth-Sci Rev, 88: 118–144
Schepers G, van Hinsbergen D J J, Spakman W, Kosters M E, Boschman L M, McQuarrie N. 2017. South-American plate advance and forced Andean trench retreat as drivers for transient flat subduction episodes. Nat Commun, 8: 15249
Skinner S M, Clayton R W. 2011. An evaluation of proposed mechanisms of slab flattening in Central Mexico. Pure Appl Geophys, 168: 1461–1474
Skinner S M, Clayton R W. 2013. The lack of correlation between flat slabs and bathymetric impactors in South America. Earth Planet Sci Lett, 371: 1–5
Stern R J. 2002. Subduction zones. Rev Geophys, 40: 1012
Stern R, Lieu W, Mantey A, Ward A, Fechter T, Farrar E, McComber S, Windler J. 2017. A new animation of subduction zone processes developed for the undergraduate and community college audience. Geosphere, 13: 628–643
Stevenson D J, Turner J S. 1977. Angle of subduction. Nature, 270: 334–336
Suárez G, Monfret T, Wittlinger G, David C. 1990. Geometry of subduction and depth of the seismogenic zone in the Guerrero gap, Mexico. Nature, 345: 336–338
Syracuse E M, van Keken P E, Abers G A. 2010. The global range of subduction zone thermal models. Phys Earth Planet Inter, 183: 73–90
Taramón J M, Rodríguez-González J, Negredo A M, Billen M I. 2015. Influence of cratonic lithosphere on the formation and evolution of flat slabs: Insights from 3-D time-dependent modeling. Geochem Geophys Geosyst, 16: 2933–2948
Tetreault J L, Buiter S J H. 2014. Future accreted terranes: A compilation of island arcs, oceanic plateaus, submarine ridges, seamounts, and con-

tinental fragments. J Geophys Res-Solid Earth, 5: 1243–1275
Thiéblemont D, Stein G, Lescuyer J L. 1997. Gisements épithermaux et porphyriques: La connexion adakite. Earth Planet Sci Lett, 325: 103–109
Tovish A, Schubert G, Luyendyk B P. 1978. Mantle flow pressure and the angle of subduction: Non-Newtonian corner flows. J Geophys Res, 83: 5892–5898
Uyeda S, Kanamori H. 1979. Back-arc opening and the mode of subduction. J Geophys Res, 84: 1049–1061
Uyeda S. 1983. Comparative subductology. Episodes, 5: 19–24
Van Avendonk H J A, Holbrook W S, Lizarralde D, Denyer P. 2011. Structure and serpentinization of the subducting Cocos plate offshore Nicaragua and Costa Rica. Geochem Geophys Geosyst, 12: Q06009
van Hunen J, van den Berg A P, Vlaar N J. 2000. A thermo-mechanical model of horizontal subduction below an overriding plate. Earth Planet Sci Lett, 182: 157–169
van Hunen J, van den Berg A P, Vlaar N J. 2002a. On the role of subducting oceanic plateaus in the development of shallow flat subduction. Tectonophysics, 352: 317–333
van Hunen J, van den Berg A P, Vlaar N J. 2002b. The impact of the South-American plate motion and the Nazca Ridge subduction on the flat subduction below South Peru. Geophys Res Lett, 29: 35-1–35-4
van Hunen J, van den Berg A P, Vlaar N J. 2004. Various mechanisms to induce present-day shallow flat subduction and implications for the younger Earth: A numerical parameter study. Phys Earth Planet Inter, 146: 179–194
van Keken P E, Hacker B R, Syracuse E M, Abers G A. 2011. Subduction factory: 4. Depth-dependent flux of H_2O from subducting slabs worldwide. J Geophys Res, 116: B01401
Vlaar N J. 1983. Thermal anomalies and magmatism due to lithospheric doubling and shifting. Earth Planet Sci Lett, 65: 322–330
Vlaar N J. 1985. Precambrian Geodynamical Constraints. In: Tobi A C, Touret J L R, eds. The Deep Proterozoic Crust in the North Atlantic Provinces. Reidel Publ Co. 3–20
Wan B, Xiao W, Windley B F, Gao J, Zhang L, Cai K. 2017. Contrasting ore styles and their role in understanding the evolution of the Altaids. Ore Geol Rev, 80: 910–922
Wu F Y, Xu Y G, Gao S, Zheng J P. 2008. Controversial on studies of the lithospheric thinning and craton destruction of North China (in Chinese). Acta Petrol Sin, 24: 1145–1174
Wu F Y, Yang J H, Xu Y G, Wilde S A, Walker R J. 2019. Destruction of the North China Craton in the Mesozoic. Annu Rev Earth Planet Sci, 47: 173–195
Xu S T, Jiang L L, Liu Y C, Zhang Y. 1992. Tectonic pattern and evolution process of the Dabie Mountains (Anhui part) (in Chinese). Acta Geol Sin, 66: 1–14
Xu Y G, Li H Y, Pang C J, He B. 2009. On the timing and duration of the destruction of the North China Craton. Chin Sci Bull, 54: 3379–3396
Yang T, Moresi L, Gurnis M, Liu S, Sandiford D, Williams S, Capitanio F A. 2019. Contrasted East Asia and South America tectonics driven by deep mantle flow. Earth Planet Sci Lett, 517: 106–116
Yogodzinski G M, Lees J M, Churikova T G, Dorendorf F, Wöerner G, Volynets O N. 2001. Geochemical evidence for the melting of subducting oceanic lithosphere at plate edges. Nature, 409: 500–504
Zhang G W, Meng Q R, Yu Z P, Sun Y, Zhou D W, Guo A L. 1996. Orogenesis and dynamics of the Qinling orogen. Sci China Ser D-Earth Sci, 39: 225–234
Zhao X X, Coe R S. 1987. Palaeomagnetic constraints on the collision and rotation of North and South China. Nature, 327: 141–144
Zheng J, Xiong Q, Zhao Y, Li W. 2019. Subduction-zone peridotites and their records of crust-mantle interaction. Sci China Earth Sci, 62: 1033–1052
Zheng Y F, Chen Y X, Dai L Q, Zhao Z F. 2015. Developing plate tectonics theory from oceanic subduction zones to collisional orogens. Sci China Earth Sci, 58: 1045–1069
Zheng Y F, Chen Y X. 2016. Continental versus oceanic subduction zones. Natl Sci Rev, 3: 495–519
Zheng Y F, Wu F Y. 2009. Growth and reworking of cratonic lithosphere. Chin Sci Bull, 54: 3347–3353
Zhou X M, Li W X. 2000. Origin of Late Mesozoic igneous rocks in southeastern China: Implications for lithosphere subduction and underplating of mafic magmas. Tectonophysics, 326: 269–287
Ziagos J P, Blackwell D D, Mooser F. 1985. Heat flow in southern Mexico and the thermal effects of subduction. J Geophys Res, 90: 5410–5420
Zhong S, Gurnis M. 1995. Mantle convection with plates and mobile, faulted plate margins. Science, 267: 838–843
Zhu R X, Chen L, Wu F Y, Liu J L. 2011. Timing, scale and mechanism of the destruction of the North China Craton. Sci China Earth Sci, 54: 789–797
Zhu R X, Xu Y G, Zhu G, Zhang H F, Xia Q K, Zheng T Y. 2012. Destruction of the North China Craton. Sci China Earth Sci, 55: 1565–1587

(Responsible editor: Lijun LIU)